Progress in Energy and Combustion Science, Volume 68, September 2018, Pages 1–28
DOI: 10.1016/j.pecs.2018.04.001

Review of arsenic behavior during coal combustion: volatilization, transformation, emission and removal technologies

Chunbo Wang[a*], Huimin Liu[a], Yue Zhang[a], Chan Zou[a], Edward J. Anthony[b*]

a School of Energy and Power Engineering, North China Electric Power University, Baoding, Hebei Province, People's Republic of China

b School of Power Engineering, Cranfield University, Cranfield, Bedfordshire MK43 0AL, UK

*Corresponding author. E-mail address: b.j.anthony@cranfield.ac.uk (Edward J. Anthony); hdwchb@126.com (Chunbo Wang).

Abstract: Growing public awareness of the environmental impact of coal combustion has raised serious concerns about the various hazardous trace elements produced by coal firing. Arsenic deserves special attention due to its toxicity, volatility, bioaccumulation in the environment, and potential carcinogenic properties. As the main anthropogenic source of arsenic is coal combustion, its behavior in power plants is of concern. Unlike mercury, arsenic behavior in coal combustion has not been subjected to systematic, in-depth research. Different researchers have reached opposing conclusions about the behavior of arsenic in combustion systems and as yet there is relatively little research on arsenic-removal technologies.

In this paper, the volatilization, transformation, and emission behavior of arsenic and its removal technologies are discussed in depth. Factors affecting the volatilization characteristics of arsenic are summarized, including temperature, pressure, mode of occurrence of arsenic, coal rank, mineral matter, and the sulfur and chlorine content of the fuel. The behavior of arsenic during oxy-fuel combustion and the effect of combustion atmosphere (O_2, CO_2, SO_2 and $H_2O(g)$) are also reviewed in detail.

In order to better understand the pathway of arsenic in a power plant environment, a particular focus in this work is the transformation mechanism of ultra-fine ash particles and the partitioning behavior of arsenic. Finally, the effects of air pollution control devices (APCDs) on arsenic emissions are examined, along with the

effectiveness of flue gas arsenic removal technologies with different kinds of adsorbents, including calcium-based adsorbents, metal oxides, activated carbon, and fly ash.

Keywords: arsenic; coal combustion; volatilization; transformation; emission; removal

Contents

1 Introduction

Although renewable and nuclear energy sources are becoming increasingly important for our future energy demand, coal combustion is still the dominant source for power generation in the energy mix in the foreseeable future. With increasing public awareness of the environmental impact of coal combustion, serious concerns have been raised regarding the emissions of various hazardous trace elements from power plants, such as mercury, arsenic, lead, and cadmium [1]. Among the most harmful elements, arsenic is receiving increasing attention due to its toxicity, volatility, bioaccumulation in the environment (enriched in biomass such as in hyperaccumulator plants [2-4]), and potential carcinogenic properties. Arsenic can affect the gastrointestinal tract, circulatory system, liver, kidneys, and skin [5]. Nearly all types of arsenic compounds are toxic, with As^{3+} being 50 times more toxic than As^{5+}. Inorganic arsenic exposure in humans is also strongly associated with lung cancer, while ingestion of inorganic arsenic can cause skin cancer [6]. Incidents on adverse health risks resulting from arsenic contamination in the environment have been reported in many countries. It has been reported that more than 3000 cases of arseniasis in villages in Guizhou (a typical area of arsenic contamination in China, which can also be found in other parts of the world) were caused by the use of locally mined high arsenic coal. In addition, arsenic is the main cause of denitrification catalyst poisoning in selective catalytic reduction (SCR) systems [7-9]. In 2011, the US Environmental Protection Agency (EPA) [10] announced the first formal nationwide regulatory standard to "limit toxic gas emissions of power plants", including an emission limitation for arsenic.

Subsequently, in 2016, the EPA [11] published the latest national emission standards for hazardous air pollutants from coal- and oil-fired electric utility steam generating units. The emission limits for arsenic in various sources are listed in Table 1 below.

Table 1: Arsenic emission limits for various sources, EPA [11]

Arsenic emission source	Emission limits for existing electric utility steam generating units (EGUs)	Emission limits for new or reconstructed electric utility steam generating units (EGUs)
Coal-fired unit not low rank virgin coal	9.08 μg/kWh	1.362 μg/kWh
Coal-fired unit low rank virgin coal	9.08 μg/kWh	1.362 μg/kWh
IGCC unit	9.08 μg/kWh	9.08 μg/kWh
Liquid oil-fired unit—continental (excluding limited-use liquid oil-fired subcategory units)	13.62 μg/kWh	1.362 μg/kWh
Liquid oil-fired unit—non-continental (excluding limited-use liquid oil-fired sub-category units)	36.32 μg/kWh	27.24 μg/kWh
Solid oil-derived fuel-fired unit	2.27 μg/kWh	1.362 μg/kWh

These strict emission limits underscore the need to study the volatility and transformation behavior of arsenic during coal combustion.

2 Arsenic in coal

2.1 Concentration of arsenic in coals around the world

The concentrations of arsenic in coals around the world are shown in Table 2. Due to the differences in post-depositional processes and coalification processes [12-17], large variations in arsenic content occur.

Table 2: Arsenic concentration in the world

Country, coal	Number of samples	Content of As in coal, μg/g	Reference
Slovakia, in Prievidza district	19	up to 1540	Keegan et al. [18]
Ukraine, the Donets Basin		32.7 average	Kizilshtein and Kolodhkov [19]
Thailand, Mae Moh Mine		3.07-515	Wongyai et al. [20]
Turkey, the Gokler coal field		170-3854	Karayigit et al. [21]
USA, the Danville Coal Member in Indiana		0.5-43	Mastalerz and Drobniak [22]
USA, the Springfield Coal Member in Indiana		1-50	Mastalerz and Drobniak [22]
USA, from the Middle Pennsylvanian Breathitt Group Fire Clay coal bed	11	1-418	Ruppert et al. [23]
Bulgaria, Dobrudza coal basin	14	2-50	Eskenazy [24]
Canada, the Elk Valley coal field		8-108	Goodarzi et al. [25]
Pakistan, two sites of Thar coalfield	40	18- 22.2	Ali et al. [26]
Greece, lignite samples from Domeniko coal deposit (Upper Miocene) in Elassona basin	38	11-40	Pentari et al. [27]
India, Makum coalfield		0.04-0.24	Mukherjee and Srivastava [28]
China, Permian-Carboniferous and Jurassic coals		0.1-94	Luo [29]
China, coals from each province	1018	4.7 average	Luo [29]
China, southwest Guizhou Province		30-534	Luo [29]
China, southwestern area		up to 35000	Ding et al. [30]

Although for most coals the average concentration of arsenic is 0.5-80 μg/g [15], some, for example those in southwestern China, have an extremely high concentration. The flue gas generated by high arsenic coals may

cause serious poisoning and deactivation of the SCR catalysts. Moreover, dispersion of arsenic-enriched fly ash can also contaminate soil and groundwater with resultant local arsenic poisoning.

2.2 Speciation of arsenic

Arsenic in coal occurs in three dominant forms: pyrite, organic, and arsenate [31-33]. Chen et al. [34] analyzed 147 Chinese coal samples from different coal-forming ages and ranks, and found that inorganic arsenic mainly occurred with sulfur in pyrite, especially as a substitute for sulfur in pyrite-type compounds [35-38]. Using chemical analyses from an electron probe micro-analyzer (EPMA), Savage et al. [39] suggested most arsenic was present in solid solution in pyrite, rather than in micro-inclusions of separate arsenic phases. Filby et al. [40] found that arsenic was always associated with inorganic elements. However, Goodarzi [41-43] suggested that for some Canadian coals arsenic had an organic association, while a strong organic association for arsenic was also suggested for a Texas lignite [44]. Factor analysis of 350 shale samples from the Illinois coal basin revealed association of arsenic with pyrite and organic matter [45].

Guo et al. [46] chose three Chinese coals to study the thermal stabilities of arsenic. Yunnan(YN) coal contained much more arsenic and sulfur than Datong (DT) and Yima (YM) coals. X-ray diffraction (XRD) results showed that the main mineral components in DT and YM coals were quartz and silicates, and in YN coal were pyrite and arsenopyrite. This was demonstrated by using scanning electron microscopy-energy dispersive X-ray (SEM-EDX) (Figure 1(a)) and Time-of-Flight Secondary Ion Mass Spectrometry(TOF-SIMS) techniques (Figure 1(b)). Note that the tested char sample was obtained after four extraction steps, in which the speciation of ion exchangeable, arsenic bound to carbonates, arsenic bound to Fe–Mn oxides and organic-bound had been removed. The arsenic remaining in the residual product included arsenic associated with detrital silicate, aluminosilicate minerals, resistant sulfur compounds, and refractory organic materials[46].

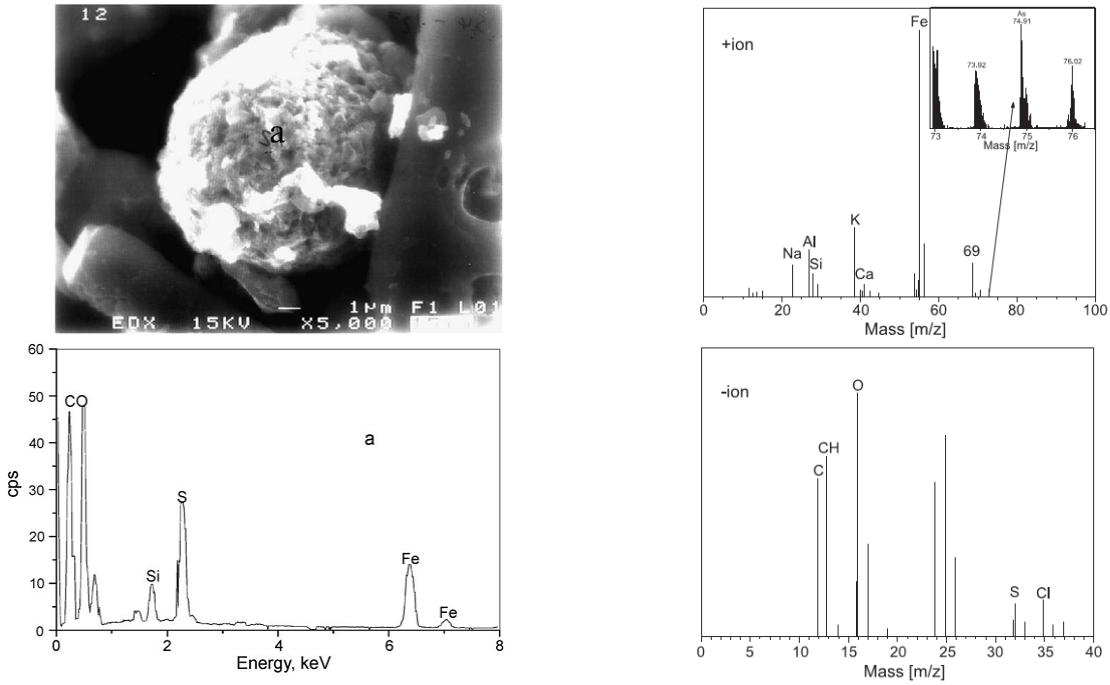

(a) SEM-EDX (b) TOF-SIMS spectrum

Figure 1: SEM-EDX results and TOF-SIMS spectrum of YN char after extraction procedure[46]

The valence state of arsenic in coal was also studied to determine its possible speciation. Zhao et al. [47] found that arsenic occurred as arsenate and arsenite, rather than in the form of sulfide or other arsenic-containing minerals. In addition, X-ray absorption near edge structure (XANES) spectrum of arsenic in a Wyodak coal sample showed that the arsenic in the coal consisted of about 50% As^{3+} (assumed to be carboxyl bound) and 50% arsenate [48]. With XANES spectroscopy, Shah et al. [49] found 65% As^{5+}, 25% As^{3+} and 10% arsenic/pyrite in a representative bituminous coal from a power station in New South Wales, Australia. For a bituminous coal in a Canadian power plant, arsenic in raw coal was reported to be dominated by arsenate (54%), arsenical pyrite (FeAsS) (24%) and an arsenite (As^{+3} -O) species (12%) [50].

Regardless of the variation of arsenic content and occurrence forms in different coals, it is generally accepted that pyrite-associated arsenic represents the major occurrence of arsenic in coal. The ratio of arsenic speciation in decreasing order is pyritic>arsenate>organic, and in terms of the valence state: As^{5+}> As^{3+}.

3 Factors affecting arsenic volatilization during coal combustion

The volatilization behavior of arsenic is closely linked to the devolatilization and char combustion processes, which are highly affected by the composition of a coal (as expressed in terms of ultimate/proximate analysis, minerals, and S and Cl content), the arsenic content in coal and the mode in which it occurs, and the surrounding environment (temperature, atmosphere, pressure) [51-56].

3.1 Temperature

Clarke [57] noted that temperature was the main factor affecting arsenic volatilization in coal. The current consensus is that the volatilization proportion of arsenic increases with temperature [46, 52, 55-60]. Senior et al. [56] reported that in bench-scale combustion experiments using bituminous and subbituminous pulverized coals, 40% to 80% of the initial arsenic content was vaporized at 1150ºC. Based on the concentrations of arsenic in the coal and bottom ash, Senior et al. [61] calculated the volatility of arsenic from eight pulverized coal power plants and found the degree of vaporization varied from 55% to 98% in the combustion zone (1400-1500ºC). In a study by Liu et al [62], seven coals with different ranks were burned in a high-temperature tube furnace and 54% to 99% of the initial arsenic in the coals was found to completely vaporize during the combustion process (1500ºC). However, Zeng [63] found that, only 36% on average of the initial arsenic in 23 coals vaporized in a laboratory-scale combustion system at 1480ºC with 20% O_2 [63].

The temperature staged volatilization characteristics of arsenic as reported in the literature [46, 52, 59, 62, 64], are given in Table 3.

Table 3: Staged volatility behavior of arsenic with temperature

Temperature range/ºC	Experimental condition	Coal samples	Staged volatility behavior	Authors
300-1000	pyrolysis	Three Chinese coals V_{ad} = 26.91% - 36.78%	500-700ºC, fastest at >700ºC, little effect	Guo et al. [46]
350-900	pyrolysis	One lignite coal (Yima coal) V_{daf} = 40.19%	350-500ºC, fast >500ºC, low	Lu et al. [59]
600-1000	combustion	High-arsenic coals V_{ad} = 6% - 30%	700-900ºC, fastest	Dai and Li [52]
300-1200	pyrolysis	Haizi (HZ) mine in southwest Guizhou 13 coals average arsenic content: 814 μg/g V_{ad} = 5.49% - 16.7%	<450ºC, fast 900-1000ºC, fast	Wei et al. [64]
600-1500	combustion	2 anthracites, 3 bituminous coals, and 2 lignite	800-900ºC one mass loss rate peak; >1000ºC another mass loss rate peak, details see Figure 2	Liu et al. [62]

V_{ad}: the content of volatile on air dried basis

V_{daf}: the content of volatile on dry ash free basis

Table 3 shows that the volatilization characteristics of arsenic are markedly different at different temperature ranges. To better describe the staged volatility behavior, the volatilization rate of arsenic was calculated over the range 25-1500ºC (where 25ºC stands for the ambient condition when no arsenic is volatilized) in the work of Liu et al. [62] (see Figure 2). For all the coals in Figure 2, two mass loss peaks of arsenic loss and three temperature zones were observed to be important: <600ºC, 600-1000ºC, and >1000ºC.

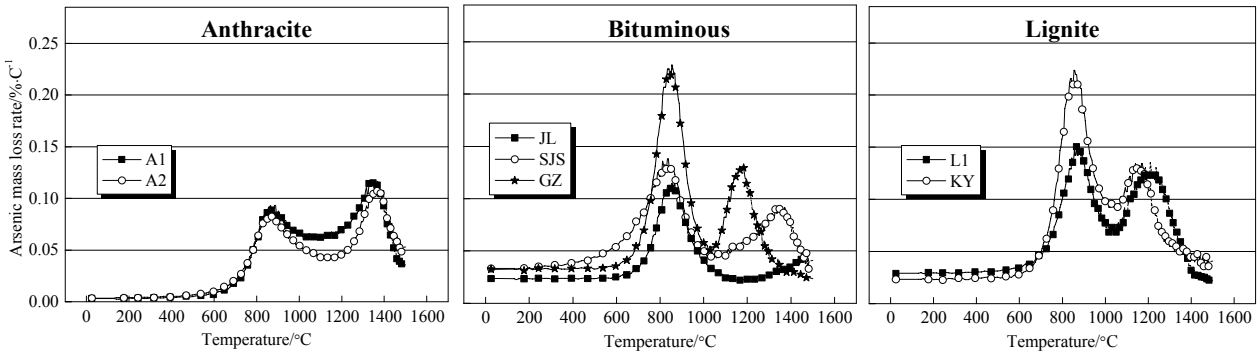

(a) anthracite (b) bituminous (c) lignite

Figure 2: Arsenic mass loss rate of different coals at 25--1500°C [62]

No consistent conclusions have been reached on the staged temperature zones (Table 3), which may be due to differences in coal type, experimental parameters and other factors. Further research is needed to determine how specific arsenic compounds behave at different temperature ranges, as well as the possible factors affecting this behavior.

Shen et al. [65] tested the temporal volatilization rate of arsenic in a fluidized bed with an on-line analysis system of trace elements in flue gas. The system allowed continuous monitoring of the vaporized arsenic based on inductively coupled plasma optical emission spectroscopy (ICP-OES). The experimental scheme is shown in Figure 3.

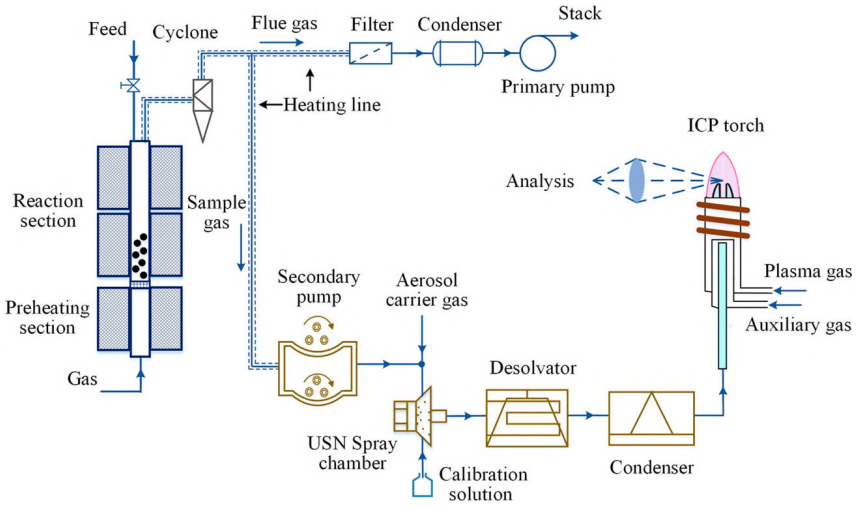

Figure 3: Fluidized bed combustor with online analysis system of arsenic in flue gas[65]

The release rate of arsenic over time is shown in Figure 4. Results showed that temperature had a significant positive effect and that as temperature increased from 600 to 850ºC, the release rate of arsenic became more rapid with a resulting higher releasing peak. At the same time, the peak time was shortened due to more intense combustion taking place. A similar phenomenon was observed by Liu et al. [66], who also studied the temporal volatilization of arsenic by changing the residence time of the raw coal.

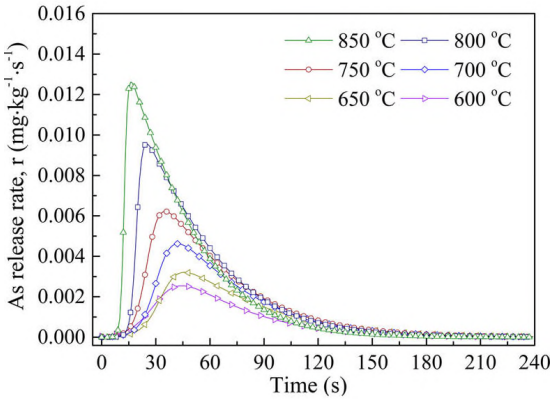

Figure 4: Release rate of arsenic from coal combustion[65]

Similarly, Wang and Tomita [55] suggested that arsenic was significantly volatilized during combustion at a rapid-heating rate of 500ºC/min, whereas only minimal quantities were emitted during combustion with a slow-heating rate of 5-10ºC/min, indicating that heating rate also affects arsenic volatilization. Moreover, to date the majority of combustion experiments have been conducted at temperatures below 1100°C due to the temperature limitations imposed by conventional tube furnaces. By contrast, the combustion temperature in a pulverized-coal boiler is generally above 1400ºC and the heating rate can be as high as 500ºC/s. This clearly indicates that further study on the effects of heating rate are required to evaluate volatilization characteristics at high temperatures and provide reference data for power plants.

3.2 Mode of occurrence of arsenic in coal

While it is clear from the above that the proportions of arsenic volatilized in coals can vary considerably in

the combustion zone (1400-1500ºC), it is reasonable to assume that this is related to the chemical speciation of the arsenic and its mode of occurrence in the coal.

In the study by Guo et al. [46], the arsenic in coals and the coal-derived pyrolysis chars were classified into five forms: ion exchangeable, carbonates-bound, Fe-Mn oxide-bound, organic matter-bound, and arsenic remaining in residue. Compared to raw coal, the decreased arsenic found in the forms bound to organic matter and bound to Fe-Mn oxides in the chars produced at 1000ºC suggested that arsenic in these forms was unstable during pyrolysis. Moreover, some of the arsenic remaining in the char residue could be expected to vaporize during pyrolysis at 1000ºC. Bool and Helble [58] reported that pyritic arsenic vaporized along with the decomposition of pyrite to pyrrhotite, and the organically-bound arsenic vaporized along with coal devolatilization. Arsenic in beneficiated Pittsburgh No. 8 coal existed partly combined with pyrite and partly in other chemical forms that were soluble in dilute HCl (including ion-exchanged arsenic)[58]. According to Liu et al. [67], arsenic in coal was divided into exchangeable, organic, sulfide and residual. With the sequential chemical extraction method [67], the modes of occurrence of arsenic in coals and ash were determined [60] and used to explain the staged volatility behavior of arsenic. Taking Kaiyuan (KY) coal (lignite, Yunnan province, China) as an example, the speciation ratios of arsenic in raw coal and ash are shown in Figure 5.

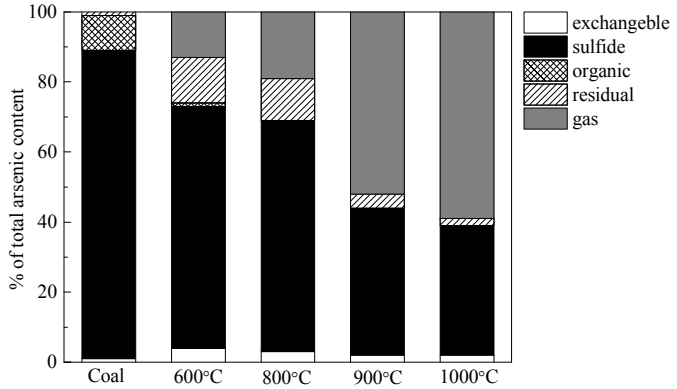

Figure 5: Speciation ratio of arsenic in raw coal and ash [60]

Using the speciation transformation results of arsenic at different temperatures in Figure 5, Liu et al. [62] concluded that arsenic that vaporized at lower than 600ºC was mainly organically bound, while arsenic vaporized at 800-900ºC was mainly due to the decomposition or oxidation of arsenic in sulfide forms. However, due to the lack of proven and reliable technology to study arsenic adsorption and the lack of temperature programming desorption similar to that available for mercury speciation determination, the specific arsenic compounds corresponding to different temperature zones have not been finally determined.

It is generally accepted that exchangeable and organic-bound arsenic are easily vaporized during the devolatilization of coal, and arsenic bound to Fe-Mn oxides and pyrite is unstable and tends to vaporize at temperatures lower than 1000ºC, while arsenates are very stable and usually decompose at relatively high temperatures. In this case, it can be expected that coals with a large proportion of unstable arsenic compounds will have higher volatilization ratios at a specific temperature, while arsenic in coals with a large number of stable arsenates is difficult to vaporize at low temperatures.

3.3 Coal rank

The effect of coal rank on the volatilization of arsenic is complex. The sequential extraction results of Liu et al. [62] indicated that coals with lower rank tended to have a higher proportion of arsenic species that more easily vaporized, which resulted in the higher arsenic volatilization ratio of lignite coals than anthracite under the same temperature conditions [62]. However, according to Senior et al. [61] who summarized the testing results of several full-scale plants equipped with different boiler types and coals, no obvious relationship was found between arsenic volatility and coal rank. For example, the vaporized fraction of arsenic was 55.2% when burning lignite while 74.3% when burning subbituminous coal based on the same tangential boiler type [61]. Liu et al. [68] studied the pyrolysis process of coal during underground coal gasification. In their work, the arsenic content

from coal to char, and coal to ash were both tested. Results discussed the two processes. For the first process (coal to char), it was found that from coal to char, arsenic volatility was highest for lignite, with bituminous coal next, and anthracite being the least volatile (Figure 6). The main reason appeared to be that lignite had the highest content of volatiles, which promoted rapid coal combustion and oxygen diffusion into the char pores, thus improving the reaction rates and trace element volatilization. For the second process (coal to ash), they suggested that over the entire volatility range from coal to char to ash, coal rank had little effect on final arsenic volatilization. As can be seen in Figure 6, the volatilization ratio of arsenic was approximately 60% for both anthracite and bituminous coal, while a smaller volatilization ratio was obtained in lignite. In the study of Liu et al. [62], instead of dividing according to coal rank, coals were divided into two groups: arsenic>4μg/g and arsenic<4μg/g. Results showed that at a given temperature the group with the higher arsenic concentration tended to have larger arsenic volatility levels.

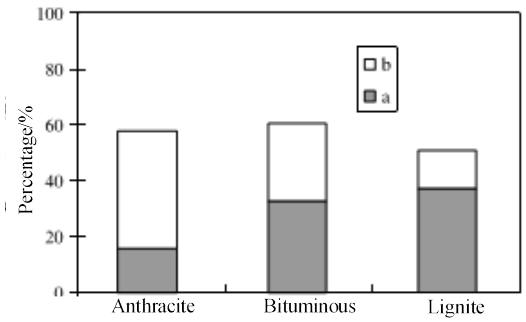

Figure 6: Comparison of volatility of arsenic during underground coal gasification of different rank of coals (a: transformation of coal to char, b: transformation of char to ash) [68]

3.4 Mineral matter

Many researchers have investigated the effects of different metallic elements (Ca, Fe, Mg, Al, Na, K and others) on arsenic volatilization and tried to develop correlations between arsenic and these elements. It is widely accepted that Ca inhibits the volatilization of arsenic [54, 58, 69-71]. Jadhav and Fan [71] studied the adsorption of arsenic in the gas phase by CaO, and determined using XRD that $Ca_3(AsO_4)_2$ and $Ca_3As_2O_7$ were formed.

However, the existence of the two compounds needs to be confirmed in future experiments. Lu et al. [59] compared the arsenic behavior in YimaD (a demineralized sample of Yima) coal with and without CaO addition. The effects of CaO on arsenic volatility are shown in Table 4.

Table 4: Effect of added CaO on the volatility of arsenic during pyrolysis of YimaD coal [59]

Temp./°C	Without CaO		With CaO		Restraining efficiency, %
	Content, $\mu g \cdot g^{-1}$	Volatility, %	Content, $\mu g \cdot g^{-1}$	Volatility, %	
600	15.2	69.2	15.5	65.4	3.8
700	16.2	69.3	18.6	59.4	9.9
800	16.3	69.4	22.4	46.1	23.4
900	15.8	72.8	21.8	58.3	14.6

It appears that the capture efficiency of CaO depended on the pyrolysis temperature and increased from 3.8% at 600ºC to 23.4% at 800ºC. This indicated that higher temperatures promoted the retention of arsenic by CaO, which was presumably caused by the formation of As–Ca compounds such as calcium arsenate. Thermodynamic analysis by Wang and Tomita [55] showed that stable $Ca_3(AsO_4)_2$ was generated at relatively low temperatures and only decomposed above 1450ºC. Experimental results obtained by Lundholm et al. [72] showed that, while the arsenic volatilization decreased when calcium was present, it was lower than that predicted by thermodynamic equilibrium calculations, which indicated transport and/or chemical reaction rate limitations.

As discussed in Section 2.2, the main chemical speciation of arsenic in coal is pyrite, suggesting that the behavior of arsenic has a close connection with iron. Some researchers have studied the capture of arsenic by mineral iron [32, 55, 58, 73, 74]. An equilibrium thermodynamic model suggested by Bool and Helble [58]

showed that the condensed arsenic species in acid (high-Si) fly ash from bituminous Pittsburgh No. 8 coal consisted mainly of $Fe_3(AsO_4)_2$, while in alkali (high-Ca) fly ash from subbituminous Black Thunder coal it appeared as $Ca_3(AsO_4)_2$. However, Yudovich and Ketris [32] suggested that iron-arsenate did not occur due to kinetic limitations, because iron was likely to be absorbed into a silicate glass. A thermodynamic analysis by Wang and Tomita [55] showed $FeAsO_4$ was generated and only decomposed above 1000ºC. In the work of Díaz-Somoano et al. [73], the equilibrium composition considering arsenic-iron interactions showed that stable $FeAsO_4$ existed at 400-800ºC. Seames and Wendt [74] studied the concentration of arsenic and iron in fly ash collected from the electrostatic precipitator (ESP) outlet in a coal-fired power plant. A strong positive relationship was found between arsenic and iron. In addition, Zhang et al. [75] conducted As_2O_3(g) adsorption experiments with different metal oxides. The results showed that the arsenic adsorption efficiency of Fe_2O_3 was around 57% and was significantly higher than for other metal oxides, also revealing that Fe_2O_3 and As_2O_3 reacted to form stable arsenates.

A correlation between arsenic and other minerals has also been reported [73, 76]. Thermodynamic results from Díaz-Somoano et al. [73] showed the formation of aluminum arsenate was possible even at high temperatures (>1400ºC) and sodium and potassium arsenates were stable below 900ºC. Magnesium arsenate was also stable from 600ºC to 1100ºC. An increase in arsenic volatility was only observed when silicon was considered in the equilibrium calculations. Contreras et al. [76] also reported that the presence of silicon had a positive effect on arsenic volatility.

3.5 Sulfur and chlorine

The content and mode of occurrence of sulfur in coal might be expected to impact arsenic volatilization. Lu et al. [59] studied arsenic volatility along with SO_2 release experiments; the results indicated that although

arsenic levels were often associated with sulfur content, especially inorganic sulfur in coal, it was difficult to correlate the volatilization behaviors of arsenic and sulfur. Some researchers have found that the volatilization proportion of arsenic was reduced in coals with higher sulfur content [77-79]. However, this conclusion is not confirmed by the necessary experimental studies. Contreras et al. [76] found the volatilization proportion of arsenic might be higher for coal with high calcium content, because sulfur was more likely to react with calcium in ash, thus reducing arsenic capture. In addition, sulfur and arsenic in coal may have competed with the active sites of CaO. However the opposite conclusions were drawn about the reaction order of $CaO+As_2O_3(g)$ and $CaO+SO_2(g)$[69, 71, 80, 81]. Moreover, some researchers mentioned that Cl or Br could also react with calcium, which could change the final effect of sulfur on arsenic[82]. To determine the effect of sulfur on arsenic volatilization, the online release curves of SO_2 were compared to the simultaneous release curve of arsenic (obtained indirectly through changing the residence time of raw coal in the tube furnace) during coal combustion in the work of Liu et al. [66]. The simultaneous volatilization characteristics of arsenic and sulfur were observed at both 900ºC and 1300ºC as seen in Figure 7, demonstrating that arsenic volatilization had a strong correlation with sulfur. Also, these authors found that coals with higher sulfur content tended to have a larger proportion of sulfide-bound arsenic, which provided support for the positive effect of sulfur on arsenic volatilization. More quantitative conclusions can be expected with the further development of online arsenic testing technology in the future.

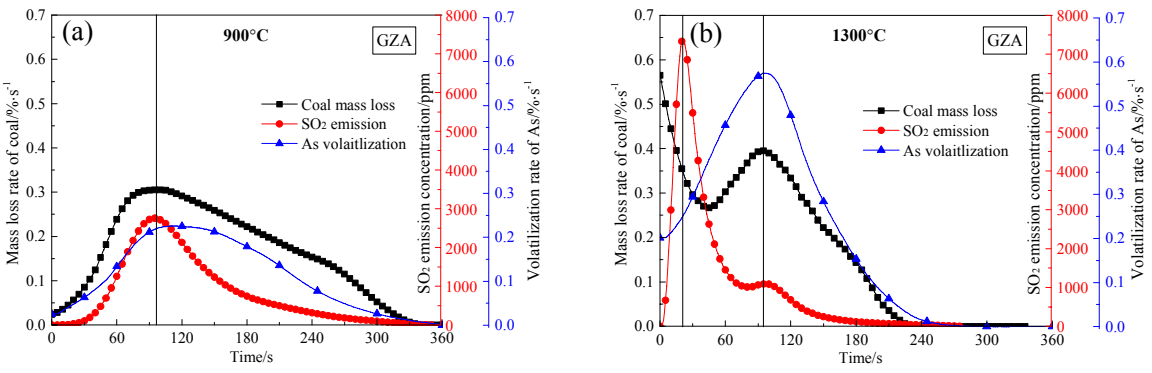

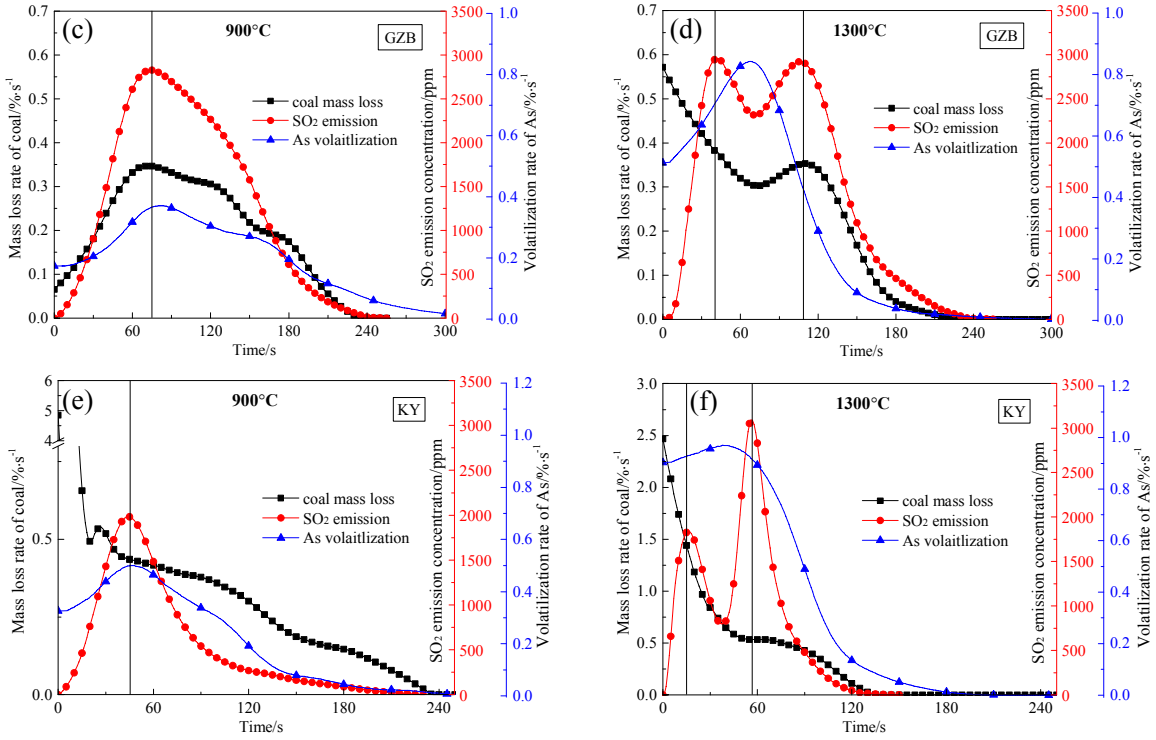

Figure 7: Simultaneous volatilization of arsenic and SO_2 during isothermal coal combustion [66] (a)GZA coal at 900ºC; (b)GZA coal at 1300ºC; (c)GZB coal at 900ºC; (d) GZB coal at 1300ºC; (e) KY coal at 900ºC; (f)KY coal at 1300ºC

Although the mechanism of decomposition of pyrite during coal combustion at different temperatures has been reported many times [83-87], the mechanism by which arsenopyrite decomposes has received relatively little attention [39, 88-90]. While possible chemical reactions regarding arsenopyrite decomposition have been simulated using thermodynamic simulation software [55], the specific reaction temperatures and reaction kinetic constant *k* value have not been reported.

In the case of the large Zhundong coal field, which has recently opened in Xinjiang province in China, the high chloride content of its coal has raised wide concern [91-97]. While chlorine can cause pipeline corrosion, a greater concern is that it may also combine with arsenic and generate highly volatile $AsCl_3$ gas. Its volatilization, and thus the study of the effect of chlorine on arsenic volatilization are of significant importance to this major project. Using thermodynamic analysis, Contreras et al. [76] found that for high-chlorine concentrations $AsCl_3(g)$ became the dominant arsenic species at 800ºC, while for low-chlorine-content fuels, $AsO_2(g)$ was the dominant

species, as shown in Figure 8. However, this study was limited to a simulation of the impact of chlorine on arsenic release and confirmatory experiments have not yet been reported.

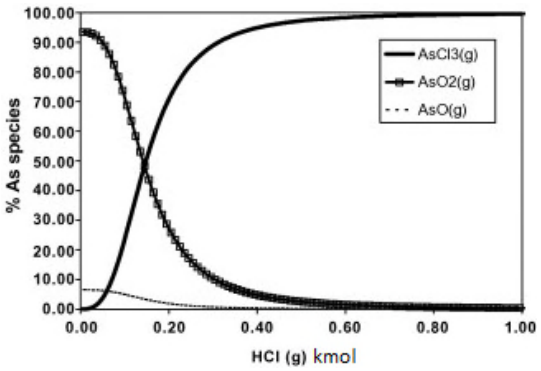

Figure 8: Chlorine effect on equilibrium distributions of major arsenic species at 800ºC [76]

3.6 Pressure

Pressure affects the flue gas equilibrium composition and may result in major changes in the proportions of equilibrium species. In the work of Liu et al. [68], high pressure was shown to lead to the formation and enhancement of the reduced species and increased condensation temperature of the volatile elements. The results of Contreras et al. [76] showed that at 800ºC, the proportion of the gaseous arsenic species increased as pressure increased, with a decrease in $AsO_2(g)$ concentration and an increase in $As_4O_{10}(g)$, as shown in Figure **9**.

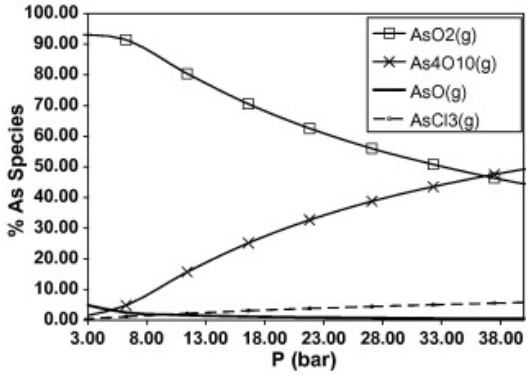

Figure 9: Equilibrium compositions for arsenic under different pressures at 800ºC [76]

The effect of pressure on arsenic components during underground coal gasification was modelled by Liu et al. [68]. Results showed that when pressure increased from 0.12 MPa to 3 MPa, the percentage of $AsH_3(g)$

increased markedly and it became the dominant species below 1250ºC, while AsH(g) was the main gas species above 1250ºC, indicating that the effect of the reducing atmosphere was enhanced at higher pressures. Moreover, the percentage of AsS(g) decreased sharply with increasing pressure, which indicated that sulfide species were not favoured at high pressures. The calculation results at 0.12 MPa and 3 MPa are shown in Figure 10.

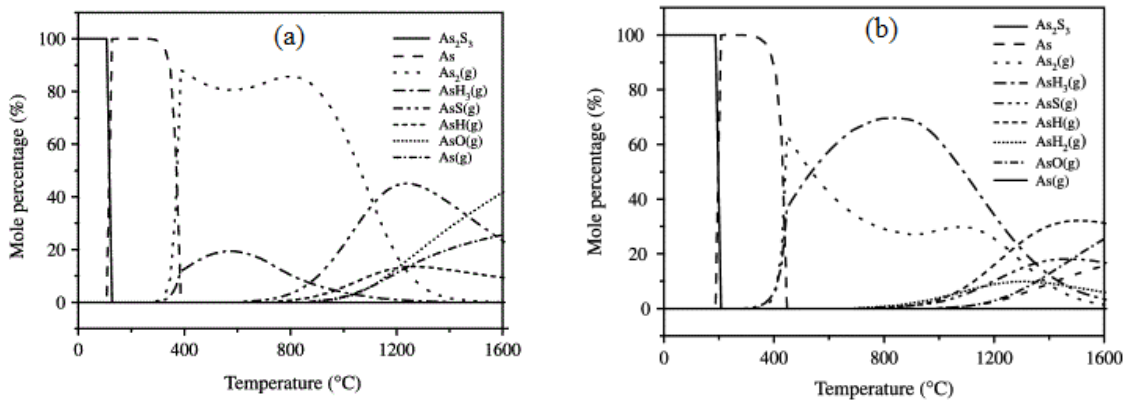

Figure 10: Equilibrium compositions of arsenic under oxygen-steam gasification (a) 0.12MPa and (b) 3MPa [68]

Overall, research on the effect of pressure on arsenic volatilization is still limited to thermodynamic simulation; and no related experiments have been reported.

3.7 Oxy-fuel combustion

Oxy-fuel combustion is a process that uses oxygen mixed with recycled flue gas for coal combustion to deliver a CO_2-rich flue gas for direct sequestration and/or storage [98, 99]. CO_2 is more easily captured under oxy-fuel conditions than in conventional air combustion and other air pollutants such as SO_2 and NO_x are reduced [100-106]. As a consequence, this technology offers near near-zero emission of air pollutants, allowing it to meet stringent emission regulations. The high CO_2 partial pressure in an oxy-fuel boiler has been hypothesized to promote higher CO levels than would be observed in conventional air-fired boilers [107, 108]; if so, this could lead to a more intensive reducing atmosphere at the surface of carbon particles, causing oxides to be reduced to unstable sub-oxides. Changes in gas composition during oxy-fuel combustion involve modification

of the operating conditions of the particle- and gas-cleaning devices compared to those in conventional air-fired pulverized coal power plants. Consequently, the physical, mineral, chemical, and leaching properties of residues (slag/bottom ash, fly ash, and flue gas desulfurization (FGD) gypsum) as well as the fate of trace elements in oxy combustion may be different from those observed in conventional air-fired power plants [109, 110]. In support of this hypothesis, Wang et al. [111] reported oxy combustion increased the concentration of trace elements measured in particulate matter (PM).

Due to the large difference between oxy and air combustion atmospheres, arsenic volatilization characteristics observed for conventional air combustion may not apply to oxy combustion. In fact, arsenic volatility during oxy combustion is strongly affected by the elevated concentrations of various gases in the boiler atmosphere, such as O_2, CO_2, SO_2 and H_2O(g).

3.7.1 O_2

Wang et al. [111] conducted an oxy combustion test at 1500ºC in a high-temperature drop-tube furnace and sampled at 135ºC to analyze the characteristics of trace elements in the particulates. This work showed that higher O_2 concentrations under oxy combustion induced lower trace element concentration in the form of fine PM. However, the work of Low and Zhang [112] showed that increased oxygen partial pressure favored the vaporization of arsenic, due to the increased particle temperature under elevated oxygen content. O_2/CO_2 combustion experiments conducted by Liu et al. [113] with a tube furnace showed that the effect of O_2 changed with temperature. At <900ºC, higher O_2 partial pressures led to more intense coal combustion and a larger volatile proportion of arsenic, irrespective of CO_2 content, while at >900ºC, the effect of O_2 was smaller. It appeared that higher O_2 partial pressure promoted arsenic vaporization and further reduced its concentration in particles.

3.7.2 CO_2

In the case of reducing conditions associated with the high concentration of CO_2 in oxy-fuel combustion, some studies have calculated the arsenic compounds produced under different excess air ratios via thermodynamic equilibrium analysis [68, 113-115]. Chatain et al. [114] found that under reducing conditions the volatilization of arsenic at 800ºC decreased due to the decrease in volatile oxides concentration. Yan et al. [115] simulated the migration of trace elements over a temperature range of 127-1527ºC with various excess air ratios from 0.6 to 1.2. They found that arsenic was easier to vaporize under a reducing atmosphere since trace elements were more likely to generate unstable compounds such as volatile sub-oxides and sulfides. Liu et al. [68] reported that the form of gaseous arsenic was mainly AsO(g) in oxidizing atmosphere at relatively high temperatures, but in reducing atmosphere As(g) became the primary species above 1450ºC. Liu et al. [113] conducted thermodynamic analysis to study the equilibrium components of calcium arsenate ($Ca_3(AsO_4)_2$) and ferric arsenate ($FeAsO_4$) with O_2/C molar ratio of 1.2 (oxidizing atmosphere) or 0.8 (reducing atmosphere), as shown in Figure 11.

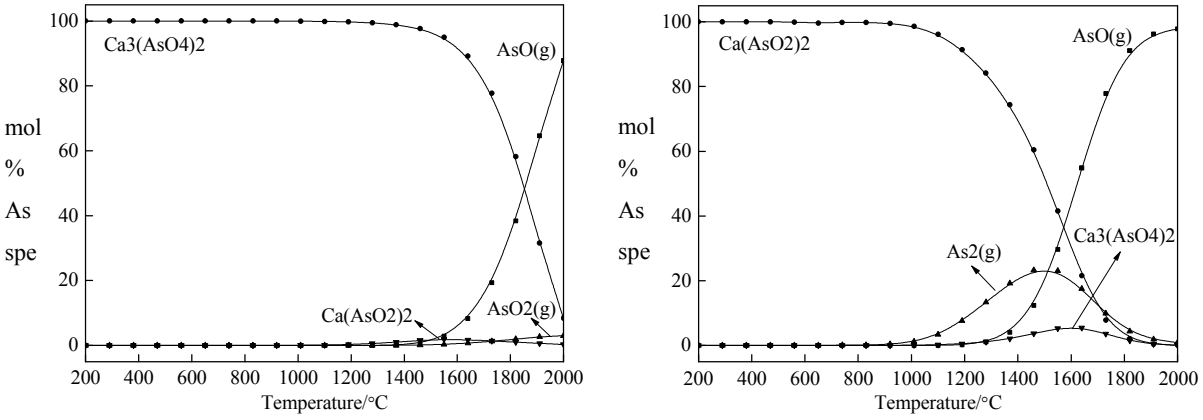

(a) $Ca_3(AsO_4)_2$ in oxidizing atmosphere

(b) $Ca_3(AsO_4)_2$ in reducing atmosphere

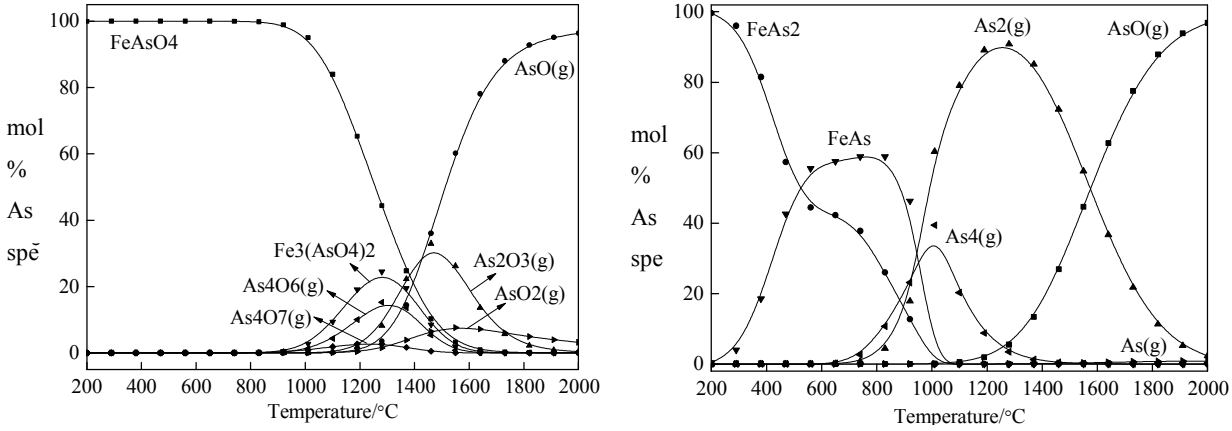

(c) $FeAsO_4$ in oxidizing atmosphere

(d) $FeAsO_4$ in reducing atmosphere

Figure 11: Equilibrium composition of arsenates in oxidizing and reducing atmospheres [113]

Figure 11 indicates that arsenic compounds with high oxidation states were reduced to compounds with lower oxidation states in a reducing atmosphere, as expected. For example, $FeAsO_4$ was reduced to FeAs and $FeAs_2$. However, the arsenic compounds with lower oxidation states had poor thermal stability, and readily decomposed into secondary oxides or elemental arsenic under high-temperature conditions [55], leading to the rapid volatilization of arsenic.

Some researchers have also studied the effects of oxy-fuel combustion on arsenic experimentally. Using a typical Chinese bituminous coal, the experiments of Wang et al. [111] indicated that oxy combustion with higher CO_2 content increased arsenic concentrations in PM as compared to air combustion, as seen in Figure 12.

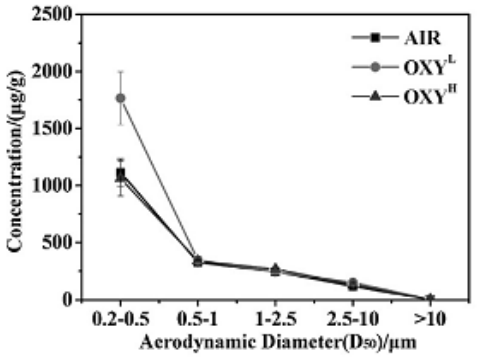

Figure 12: Arsenic concentration in various PM fractions under air combustion and oxy-fuel combustion with different oxygen concentrations. (oxy^L: 21% O_2/79% CO_2 oxy^H: 29% O_2/71% CO_2) [111]

Low and Zhang [112] did pyrolysis experiments in N_2 and CO_2 atmospheres in a lab-scale drop-tube furnace at 1500ºC to study the effect of CO_2 on arsenic behavior. The results are shown in Figure 13. The substitution of N_2 by CO_2 for oxy-fuel combustion caused little change to the emission and speciation of arsenic at the initial step of coal combustion and pyrolysis.

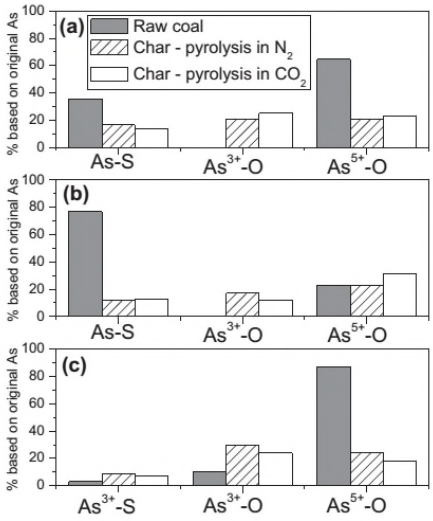

Figure 13: Evolution of As speciation upon pyrolysis of (a) DBC (bituminous coal from Datong, China), (b) Brazilian lignite and (c) As-doped VBC (brown coal from Victoria, Australia) in pure N_2 or CO_2 [112]

Roy et al. [116] simulated the equilibrium composition of arsenic compounds of three lignites under oxy combustion atmosphere using FactSage software. The results showed that at low temperature the distribution of toxic arsenic species in oxy-fuel combustion was almost the same as in air combustion. Contreras et al. [117] simulated the arsenic evaporation characteristics for different CO_2 concentrations under oxy combustion atmosphere using HSC Chemistry software [118] and also found arsenic vaporization did not increase under oxy-firing.

Zhuang and Pavlish [119] studied the behavior of hazardous air pollutants in a 200-kW oxygen-fired coal combustion power plant with different flue gas recycling (FGR) systems, as shown in Figure 14.

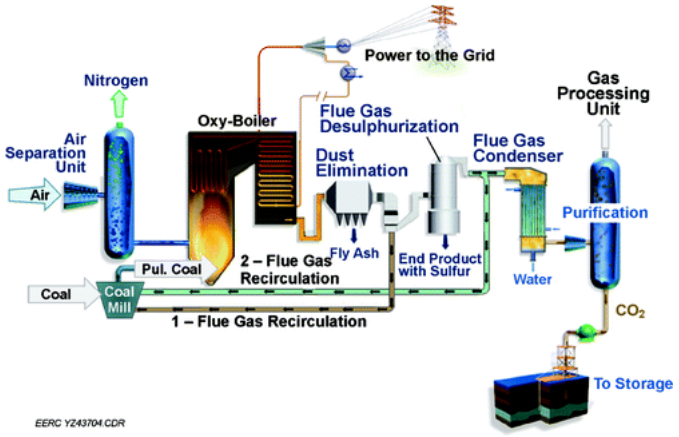

Figure 14: A 200 kW oxygen-fired coal combustion power plant with two different scenarios of FGR [119]

In contrast to Wang et al. [111], who found that higher CO_2 content increased arsenic concentrations in PM with diameter in the micrometer range, Zhuang and Pavlish [119] reported that compared with air firing, arsenic showed lower concentrations on fly ash during 21% O_2/79% CO_2 combustion with the recycled flue gas coming from the ESP outlet or the wet scrubber outlet (Figure 15), which indicated that oxy combustion increased the arsenic volatilization.

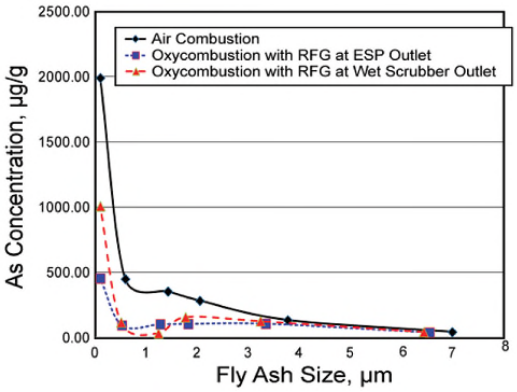

Figure 15: Comparison of arsenic size distributions under air combustion and oxy-coal combustion [119]

Currently, it is difficult to determine whether CO_2 has a positive or negative role in arsenic volatilization under oxy-fuel combustion and it is clear that further study is needed.

3.7.3 SO_2 and H_2O(g)

Wang et al. [111] reported the effects of SO_2 and H_2O on trace element distribution under oxy combustion atmosphere at 1500ºC. The results are shown in Figure 16. SO_2 reduced the total amount and concentration of trace elements in PM under oxy combustion, while H_2O(g) enhanced both the mass of the PM, and the trace element mass in the PM. The results indicated that SO_2 promoted the volatilization of arsenic during oxy-fuel combustion, while H_2O(g) reduced it.

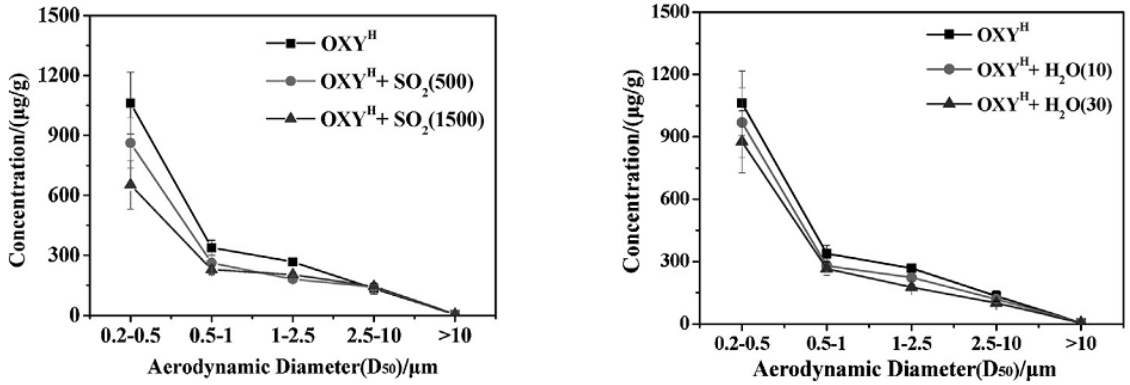

Figure 16: Concentration distribution of arsenic in PM fractions under oxy-fuel combustion with different SO_2 and H_2O(g) concentrations. OXY^H + SO_2(500) is 29% O_2/71% CO_2 with 500 ppm SO_2; OXY^H + SO_2(1500) is 29% O_2/71% CO_2 with 1500 ppm SO_2; OXY^H + H_2O(10) is 29% O_2/10% H_2O/61%CO_2; OXY^H + H_2O(30) is 29% O_2/30% H_2O/41% CO_2 [111]

However, given that only limited information is available on the effect of SO_2 and H_2O(g) on arsenic volatilization during oxy-fuel combustion, more research is needed on this subject.

The coal particles burned in circulating fluidized bed (CFB) boilers are larger than those in pulverized coal boilers and it is known that particle size is an important factor during coal combustion since it affects the ignition, burnout of coals and PM formation, as well as the volatilization of arsenic. Unfortunately, the effect of particle size on arsenic volatilization is still largely unstudied.

4 Transformation of arsenic during post-combustion

Volatile arsenic compounds in the flue gas gradually condense as the temperature decreases. Some volatile arsenic components may condense on the surface of fly ash, react with substances in fly ash, or be absorbed by

fly ash and captured by the ESP. Only a small amount of arsenic passes through the FGD system and is finally emitted to the atmosphere. Once combustion gases are carried downstream from the combustion zone of a coal-fired boiler, the key factors affecting the final trace constituent transformation/partitioning behavior are the conversion of vaporized components into various solid forms and their collection along with the fly ash. Gaseous arsenic will experience adsorption, condensation, and chemical transformation as the flue gas cools [15, 120].

4.1 Distribution of arsenic in power plants

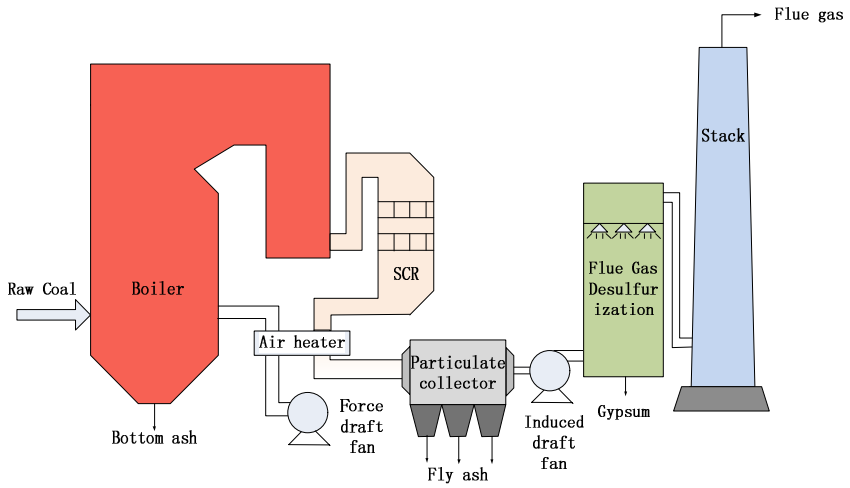

Figure 17: A typical pulverized coal combustion system and related equipment

Figure 17 shows a typical pulverized coal combustion system and related equipment. A summary of the data on the distribution of arsenic in raw coal, ash, and flue gas from such a system is presented in Table 5.

Table 5: Distribution of arsenic in power plants

Power Plants	Coal	Raw coal µg/g	Bottom ash µg/g	ESP/FF fly ash, µg/g	Flue gas, µg/m^3	Balance	Source
A Brazilian power plant (Presidente Me ´dici Power Plant or UTPM-446 MW)	A high ash feed coal (A_d: 49.7%, Var: 23.1%)	4.4	1.8	11.5	----	----	Pires and Querol [121]
Shizuishan Power Plant	V_{daf}: 30.62; A_d: 39.32%	5.35	1.59	5.67	----	----	Song et al. [122]

Two Finnish coal-fired power plants	Plant SB, Var: 29.4%	4.1	<10	39	----	125%	Aunela-Tapola et al. [123]
	Plant HB, Var: 29.6%	6.3	5.2	32	----	113%	
Two 660 MW boilers with a low-temperature economizer (LTE)	A mixed coal: Var:31.02% S: 2.38%	16.42	0.304 based on the initial coal	9.093 based on the initial coal	----	57.30%	Wang et al. [124]
An underfed stoker unit with approximately 50 kW capacity 1100-1250ºC	Var: 9.26%	1.6	7.9	31	Nd	27%	Li et al. [125]
	Var: 36.44%	4.3	11	46	Nd	36%	
	Var: 37.18%	1.4	2.4	18	Nd	22%	
CFB, 50 kW Waikato coal	Ad: 3.5%	0.86	5.5	11	38	----	Clemens et al. [126]
			5.9	9.5	33		
			4.8	8.9	34		
1400 MW coal-fired power	A_d: 27.3%	45.7	10.4	169.6	18.4	79.1%	Otero-Rey et al. [127]
	A_d: 22.3%					64.4%	
	A_d: 22.8%					60.2%	
220 MW installed capacity and equipped with tangential burners	A_d: 34.67%	41.9±2.4	172.3±12.3	9.8±1.7	19.5±2.4	83.47%	Reddy et al. [128]
	A_d: 32.51%					84.20%	
	A_d: 36.25%					83.26%	
Three 440t/h CFB with ESP/FF and WFGD Petroleum coke and coal blends	Var: 22.40%, Aar: 16.8%	3.79	21.80	23.30	0.97	114.2%	Duan et al. [129]
	Var: 18.07%, Aar: 11.41%	3.05	36.60	13.64	0.32	80.0%	
	Var: 18.07%, Aar: 11.41%	3.05	29.00	17.25	0.31	86.0%	

A_d: ash content in coal on dry basis; V_{ar}: volatile content in coal on as received basis; V_{daf}: volatile content in coal on dry ash free basis; Nd: not found; ----: not measured.

Many researchers have calculated the mass balance ratio of arsenic by measuring the arsenic concentration

in solid products, without considering the gas phase. In the work of Aunela-Tapola et al. [123], two Finnish coal-fired power plants (SB and HB) were experimentally investigated with regard to the distribution of arsenic. The mass balances of arsenic in two bituminous coals in SB and HB, were 125% and 113%, respectively. Only 22% to 36% arsenic recovery was obtained by Li et al. [125] when testing three lignites. For a mixed coal in two 660 MW boilers with a low-temperature economizer (LTE), the mass balance of arsenic was only 57.3% [124]. The relatively low mass balance of arsenic was mainly due to arsenic in the flue gas and ultrafine particles (<0.2 μm) not being accounted for. Unlike laboratory experiments, the sampling process in an industrial system can experience significant deviation; hence, these mass balance values must be considered acceptable. Moreover, mass imbalances may arise because arsenic can condense or be absorbed on interior surfaces of equipment such as heating surfaces [130].

Only a few researchers have studied the mass balances of arsenic considering both solid and gaseous arsenic. Clemens et al. [126] studied Waikato coal under fluidized bed combustion (50-kW capacity). Although this study took the gaseous arsenic into account, it did not give the specific mass balance figures. The arsenic concentration in flue gas was 18.4 μg/m^3 in the work of Otero-Rey et al. [127], where 60.2% to 79.1% of arsenic mass balance was obtained. Reddy et al. [128] researched the emission characteristics of arsenic at a 220-MW power plant equipped with tangential burners burning three types of coal with arsenic content of 41.9±2.4 μg/g. The mass balance of arsenic in the three coals was in the range of 83.26% to 84.20%. However, the arsenic balance considering all phases was lower than 100%; one possible reason is that the sampling of arsenic in flue gas was not done using online sampling techniques. Here, the sampling method was liquid sampling, using absorption bottles. During flue gas sampling, the flue gas was cooled continuously as it passed from the flue into the absorption bottle, which may have caused some of the arsenic in the flue gas to condense on the pipes.

However, the metal inner wall of the sampling gun could not be acid washed, which likely resulted in the loss of arsenic in the gas phase. In general, such problems ensure that the mass balance results of arsenic considering the gas phase are typically much less than 100% [127, 128].

4.2 Enrichment of arsenic on fine particles

Trace elements can be categorized into three main groups with regard to their partitioning during coal combustion [13, 57, 131-137]. Elements such as As, Cd, Pb, Sb, and Se are in group II and are found concentrated more on the fine-grained fly ash particles [31]. Thus, most of the generated arsenic vapor is captured by fly ash and tends to accumulate on the surface of the smaller particles of the fly ash, which here refers to those particles whose aerodynamic diameter is less than 10 μm [138-144].

Querol et al. [145] tested the content and distribution of 23 trace elements in the fuel (organic and/or inorganic affinities) and in the combustion wastes (partition and volatility) during combustion in a large power station. Results showed that arsenic exhibited segregation in the fly ash (fly ash/slag concentration ratio > 1.5). Likewise, Liu et al. [146] found that while the arsenic concentration in the feed coal of a coal-fired power plant in the Yanzhou area of Shandong was only 2.3 μg/g, arsenic concentration was three times higher in the fly ash (7.0 μg/g). Zhao et al. [53] reported a bimodal distribution of arsenic associated with particulates during the combustion of high-arsenic coals from the Guizhou province of China. When the temperature increased from 1100°C to 1400°C, an emission of arsenic in PM with diameter less than 1μm (PM1) increased from 0.07 mg/Nm^3 to 0.25 mg/Nm^3. Based on the enrichment factor proposed by Ratafia-Brown [147], Tang et al. [148] tested the enrichment factors of arsenic in fly ash collected from four hoppers in one of the utility boilers from the Luohe Power Plant (LH#1), in Anhui Province, China (as shown in Figure 18). From electric field 1 to electric field 4, the enrichment factors of arsenic increased sharply from 0.6 to 4.4, indicating that arsenic tended

to be enriched in smaller particle sizes.

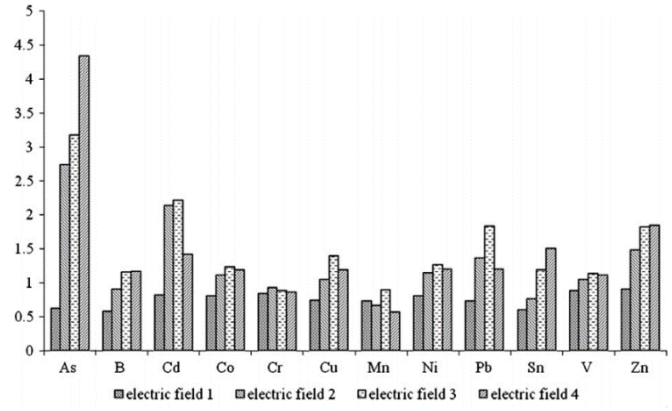

Figure 18: Variation of enrichment factors in fly ash collected from four hoppers at the LH#1 boiler [148]

Studies of arsenic partitioning conducted over the past 40 years have been focused on the enrichment of arsenic in the submicron fly ash particulate. The findings of these studies are reported in Table 6.

Table 6: Arsenic enrichment in submicron fly ash particulate grouped by coal type and the size of the facility

Coal type/source	Boiler size	Method	Source
Field studies			
B Ill./Ky.	290 MWe	[c] FA BA	Klein et al. [149]
B U	350 MWe	[c] f(dp), ESP-O	Gladney et al. [150]
B Poland	17.2 kg/s	[c] FA BA	Kauppinen and Pakkan [151]
B US, Austral.	115-645 MWe	RE FA BA	Meij et al. [120]
S Spain	1050 MWe	[c] f(dp), ESP ash	Querol et al. [13]
B UK	2000 MWe	[c] FA BA	Martinez [152]
B Illinois	U	RE FA BA	Demir et al. [153]
B Poland	160, 113 MWe	RE FA BA	Aunela-Tapola et al. [123]
B Netherlands	600 MWe	[c] FA BA	Sandelin and Backman [154]

B Finland	560 MWe	[c] FA BA	Sandelin and Backman [49]
U Slovakia	U	[c] FA BA	Keegan et al. [18]
B China	U	[c] FA BA	Liu et al. [146]
B India	220 MWe	[c] FA, BA	Reddy et al. [128]
U China	300 MWe	[c] FA BA RE	Guo et al. [155]
B Australia	660 MWe	[c] FA BA	Shah et al. [49]
B U	795 MWe	[c] FA BA ESP-I	Cheng et al. [156]
B Indian	U	[c] FA BA	Pandey et al. [157]
U	U	[c] FA BA RE ESP	Córdoba et al. [158]
U Brazil	857 MWe	[c] FA BA	Quispe et al. [159]
U Balingian	U	[c] FA BA	Sia and Abdullah [160]
U China	300, 600 MWe	[c] FA BA RE	Tang et al. [70]
U China	U	[c] f(dp)	Jin et al. [142]
U China	U	[c] FA BA RE	Tang et al. [148]
U China	U	[c] FA	Hu et al. [161]
Laboratory- and pilot-scale studies			
L North Dakota	Lab 17 kW	RE f(dp)	Linak and Peterson [162]
U	90 kW_{th} oxy combustion pilot plant	[c] FA BA	Font et al. [163]
A, B China	2.5 MW CFB combustor	[c] f(dp) FA BA	Lunbo et al. [164]
Bench-scale (drop-tube) studies			

B, S, L US	20% O_2	RE f(dp)	Quann [165]
B Illinois (b)	10.5% O_2	[c] f(dp)	Helble [166]
B, S Pitt., Wyo.	SR 1.2	[c] f(dp)	Bool and Helble [58]
L Montana	20% O_2	[c] f(dp)	Neville and Sarofim [167]
B USA	SR=1.2/0.9	[c] f(dp), FA	Senior et al. [56]
A, B China	20% O_2	[c] f(dp), FA	Zhao et al. [53]
A, B China	50% O_2	[c] f(dp), FA	Zhao et al. [53]
B Australia	21% O_2	[c] FA	Jiao et al. [168]

B, bituminous; S, subbituminous; L, lignite; Br, brown coal; BA, bottom ash; FA, fly ash; ESP-I, ESP inlet; ESP-O, ESP outlet; U, unspecified. [c] FA BA means in the literature the concentrations of fly ash and bottom ash were tested. [c] f(dp) means concentration measured as function of particle size. RE, relative enrichment factor as defined by Meij et al. [120]. Table represents expansion of studies summarized by Helble [169]

4.2.1 Factors affecting arsenic enrichment

Effect of temperature. Quann et al.[170] studied the size distribution of fly ash at 1780ºC and 2180ºC. The amount of submicron aerosol increased markedly from 4% of total fly ash at 1780ºC to 20% at 2180ºC, showing that increasing temperature enhanced the formation of submicron aerosol particles. Results supported the hypothesis that the enrichment of the smaller ash particles in more volatile species such as arsenic was due to a process of vaporization and re-condensation of mineral constituents. Senior et al. [171] showed flame temperature had a dramatic impact on the amount of certain trace elements such as arsenic and selenium in the submicron ash, indicating that these elements vaporized during the combustion process. However, the amount of vaporization was not sensitive to the coal grind. In the work of Seames and Wendt [74], size-segregated ash-laden aerosol samples were isokinetically collected to study the correlations between arsenic and major elements (as functions of particle size); results showed increasing combustion temperature increased the

availability of active sites and the partitioning of arsenic and selenium onto fly ash particles.

Effect of minerals. Senior et al. [172] concluded that the composition differences among size-segregated coal samples of different density were mainly due to the density differences between minerals, especially pyrite, and the organic portion of the coal. The high-density fractions were enriched in pyrite or substances associated with pyrite. According to the experiment results of Senior et al.[172], arsenic and iron were concentrated in the high-density fraction of 45-63-mm particle size cut of Pittsburgh coal. In addition, it has been reported that the calcium present in fly ash may interact with arsenic vapor, resulting in the enrichment of arsenic [69]. Chemical associations between arsenic and calcium or iron were inferred by Seames and Wendt [74] through PM sampling with a Berner low-pressure impactor in a 17-kW downflow laboratory combustor. The correlation between arsenic and calcium/iron in ash particles is shown in Figure 19 [74], which indicates that both iron and calcium could provide sites for arsenic association.

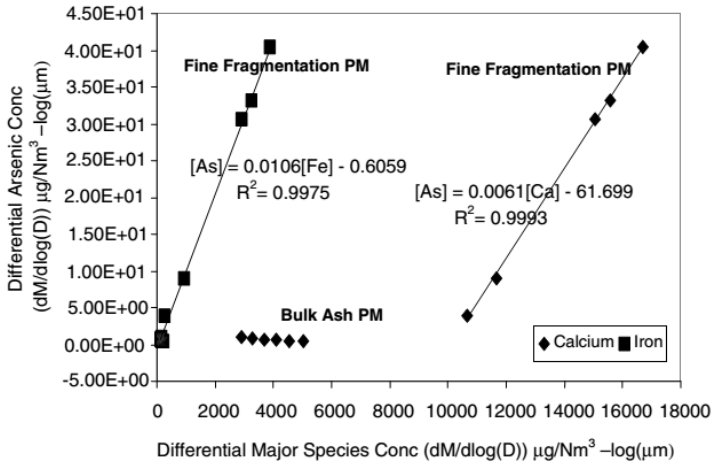

Figure 19: Typical differential distribution cross correlation result: arsenic in ash particles versus calcium and iron (Pittsburgh coal) [74]

Competition of sulfur and arsenic. Seames and Wendt [74] tested the effects of sulfur on arsenic partitioning in a 17-kW vertical downflow combustor with 2 kg/h coal premixed with air (stoichiometric ratio, SR = 1.2). Doping SO_2 with the primary combustion air, the total arsenic concentration recovered on particles during

Kentucky coal combustion, <0.973, 0.973-1.96, 1.96-3.77, and 3.77-7.33 μm in size, pooled together, decreased from a total of 695 μg/m^3 (no added SO_2) to 78 μg/m^3 (with SO_2 addition). Figure 20 shows the transformation of arsenic compounds with sulfur in coal. Sulfur was thought to compete with these surface reactions of minerals and arsenic, which decreased arsenic partitioning onto fly ash surfaces.

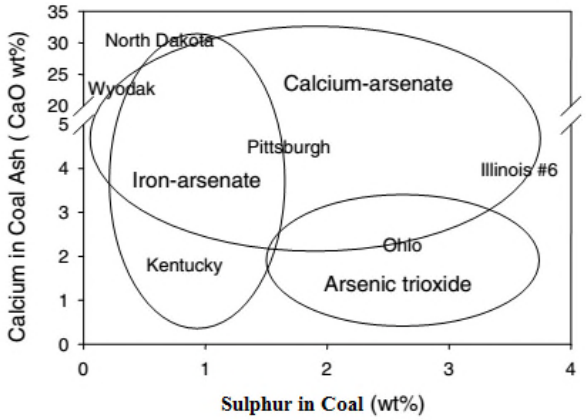

Figure 20: Regimes for arsenic speciation during pulverized coal combustion [74]

Equipment (Low-temperature economizer(LTE)). Wang et al. [124] measured PM and trace elements from a coal-fired power plant with ESP, equipped with a Low-temperature economizer (LTE). The enrichment factors of trace elements in $PM_{0.2\text{-}0.5}$ (diameter range 0.2-0.5μm) were markedly higher than those of $PM_{0.5\text{-}1.0}$ (diameter range 0.5-1.0μm), showing arsenic tended to be enriched in fine particles. Particularly, with the LTE operating, the enrichment factor of arsenic in $PM_{0.2\text{-}0.5}$ decreased sharply from 42 to 32, as shown in Figure 21. A possible reason is that with the LTE on, a lower flue gas temperature (100-108ºC) was obtained than with the LTE non-operational (138-146ºC), which significantly reduced the amount of PM at the outlet of the ESP. As a result, the concentration of arsenic in fine PM was reduced. In addition, the decreasing enrichment factor order of trace elements (As>Cd>Cr>Pb>Mn) indicated that trace elements with higher volatility had an increased enrichment in the fine particles [120, 173, 174].

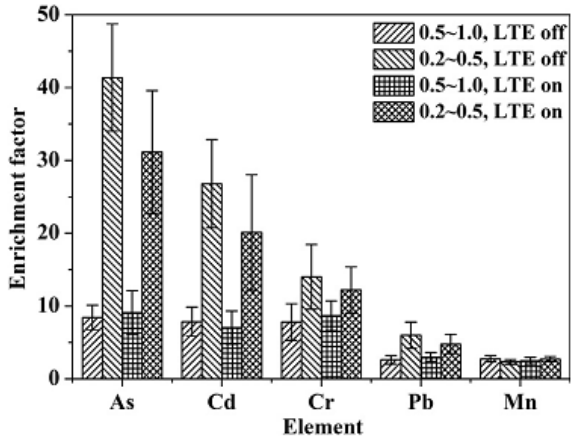

Figure 21: The enrichment factors of trace elements in $PM_{0.5\text{-}1.0}$ and $PM_{0.2\text{-}0.5}$[124], where LTE is Low-temperature economizer

Difference between bench- and pilot-scale results. The concentration of arsenic in submicron particles at the ESP inlet emphasized the difference between pilot-scale tests and laboratory results, as shown in Figure 22 [171]. According to Senior et al. [171], the amount of ash in the vaporization mode as well as the amounts of several refractory elements (Ca, Fe, and Co) in the laboratory combustor [56] were similar to the pilot-scale study [171]. Thus, they concluded that the flame conditions in the two systems were similar. In this case, the results of laboratory and pilot-scale tests were compared to study the transformation of arsenic. In the laboratory sample at 1150ºC, 25% of arsenic was found in the submicron mode, while in the submicron sample from the pilot-scale combustion facility less than 5% of arsenic was found. The possible reason is that more chemical condensation took place in the pilot-scale test, which caused arsenic present in the gas to condense preferentially on larger ash particles, not on the submicron ash.

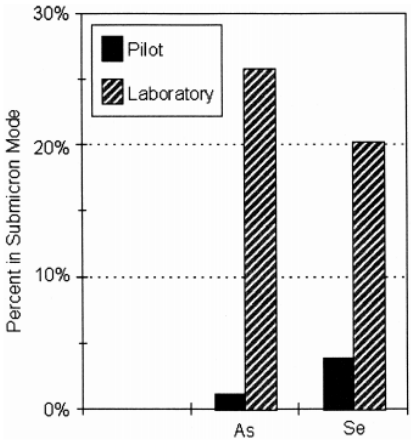

Figure 22: Comparison of As and Se in the submicron mode from the laboratory combustor sampled at 1150ºC [56] and the pilot combustor sampled at the ESP inlet [171]

Arsenic enrichment in fine ash is affected by many factors. Further studies are needed to obtain consistent conclusions on the effect of each factor, as well as the reactions between arsenic and fly ash. In addition, the available fly ash surface area for arsenic condensation/adsorption is also required information for the purpose of predicting the partitioning of arsenic, thereby reducing toxic emissions in combustion systems.

4.3 Speciation transformation of arsenic

Total concentrations of trace elements in raw coal and ash samples and their partitioning in coal-fired power stations have been extensively studied in the last few years, with diverse analytical methods [175]. Speciation of individual trace elements, however, requires more specific analytical measurement techniques, which are significantly different from those applicable to the determination of total elemental concentration [139, 176-182]. X-ray absorption fine structure (XAFS) spectroscopy has been widely used to determine the speciation of trace elements in solid phases [88, 183]. In recent years, XANES and extended X-ray absorption fine structure (EXAFS) spectroscopy, which are more sensitive to the local structural environment of an element, have begun to be used in speciation studies of trace elements.

Arsenic XANES and arsenic EXAFS spectra by Zielinski et al. [139] indicated that most arsenic in the coal

was contained in a generation of arsenic-bearing pyrite (arsenian pyrite (FeS_2-As), arsenopyrite (FeAsS), or As substitutes for S in pyrite ($Fe(As_xS_{1-x})_2$)), while most (95%) of the arsenic was present as As^{5+} in fly ash. The majority of arsenic in a highly alkaline (pH = 12.7) fly ash was present as As^{5+} in calcium arsenate ($Ca_3(AsO_4)_2$). While in a highly acidic (pH = 3.0) fly ash, arsenic was associated with some combination of iron oxide, oxyhydroxide, or sulfate. Shah et al. [49] tested the arsenic speciation in feed coal and combustion products. In coal 65% As^{5+}, 25% As^{3+} and 10% As/pyrite were found, while in the fly ash, 90% of arsenic was found as the less toxic As^{5+} and 10% as As^{3+}. The arsenic XANES spectra of coal and fly ash samples determined by these workers are shown in Figure 23. This finding is consistent with the previous studies that arsenic in fly ash was mainly present as As^{5+} with lower concentrations of As^{3+} [184-186]. This was partly caused by the interaction of As_2O_3(g) in the As^{3+} form with CaO in fly ash, which formed the stable As^{5+} compounds [76, 81, 187-189].

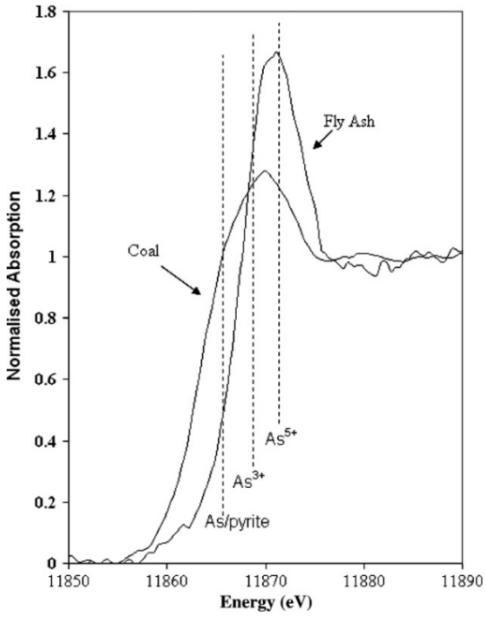

Figure 23: Arsenic XANES spectra of coal and fly ash samples [49]

In the work of Goodarzi et al. [50], a medium volatile bituminous coal with an ash content of 34 wt.% was combusted in a 150-MW Canadian power plant. The distribution of arsenic in feed coals, ash, and stack-emitted materials was determined with XANES spectroscopy. Results showed, first, that arsenic in the feed coal was

dominated by arsenate (54%), followed by arsenical pyrite (FeAsS) (24%) and an arsenite (As^{3+} –O) species (12%) (Figure 24(a)). It is possible that the As^{5+} and As^{3+} species were derived by oxidation of the arsenical pyrite [180]. Second, the content of arsenic in bottom ash was quite low, while a majority of arsenic (>90%) in fly ash was present as As^{5+} (as shown in Figure 24(b)). Third, more than 99% of total arsenic was captured by the particulate removal devices.

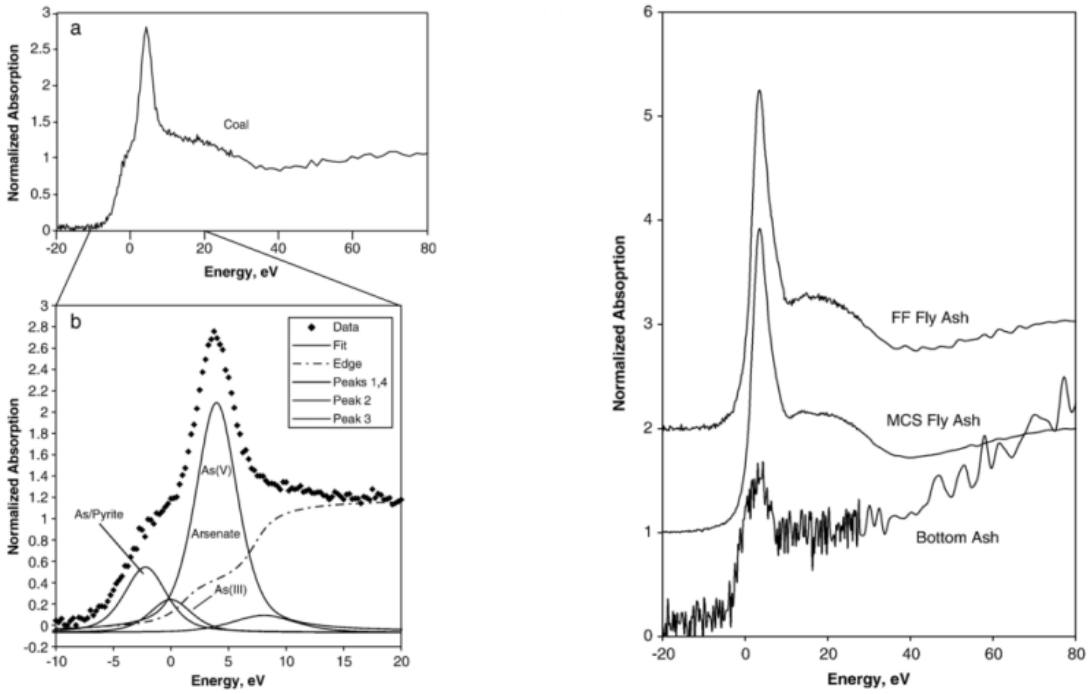

(a) milled coal **(b) ash samples from power plant**

Figure 24: Arsenic XANES spectrum of milled coal and ash samples from power plant. Zero-point of energy corresponds to 11,867 eV[50]

In the work of Luo et al. [141], both arsenic K-edge XANES and EXAFS spectra were collected for the speciation determination in five fly ash samples. A comparison of arsenic K-edge XANES spectra of the samples to spectra of oxidation-state standards demonstrated that arsenic was predominantly As^{5+} in all samples. Furthermore, mansfieldite ($AlAsO_4 \cdot 2H_2O$) [190], calcium arsenate [$Ca_3(AsO_4)_2$] [191], and calcium pyroarsenate ($Ca_2As_2O_7$) [192] were considered as the possible As^{5+} speciation in fly ash.

An improved graphite furnace atomic absorption spectrometry(GFAAS) method, complemented by thermal

gravimetric analyzer/differential scanning calorimeter(TGA/DSC) experiments, was first used to study trace element partitioning from mineral exclusions by Raeva et al. [193]. However, this method had limitations for trace element and inorganic matrix speciation because samples had to be introduced into the furnace in a homogeneous form. Thus water-insoluble matrices, e.g. quartz and pyrite, could not be tested.

According to the studies noted above, most of the arsenic in ash was present as As^{5+}. With regard to the arsenic speciation in flue gas, Germani and Zoller [194] concluded that the arsenic was mainly present as As_4O_6 by measuring the As_4O_6 and As^0 in flue gas. Here, 0.7 to 52% of the total in-stack concentration of arsenic in the vapor phase was reported as As_2O_3 by Ratafia-Brown [147].

4.4 Transformation mechanism

4.4.1 Fly ash formation and particle size distribution

The transformation behavior of arsenic is closely related to fly ash formation, particle size distribution, and migration evolution of minerals. The fundamental formation mechanism of coal ash is shown in Figure 25 [195]. The process was divided into two parts: coal with included minerals; and coal with excluded minerals. Residual ash ranging from 1-100 μm was formed from excluded minerals or fusion of included minerals. Sub-micron ash ranging from 0.01-1 μm was formed by vaporization, followed by homogeneous condensation, heterogeneous condensation, coagulation and aggregation, or extensive fragmentation of minerals. The size distribution of fly ash particles was thought to be influenced by several factors, including combustion environment, coal properties, and residence time.

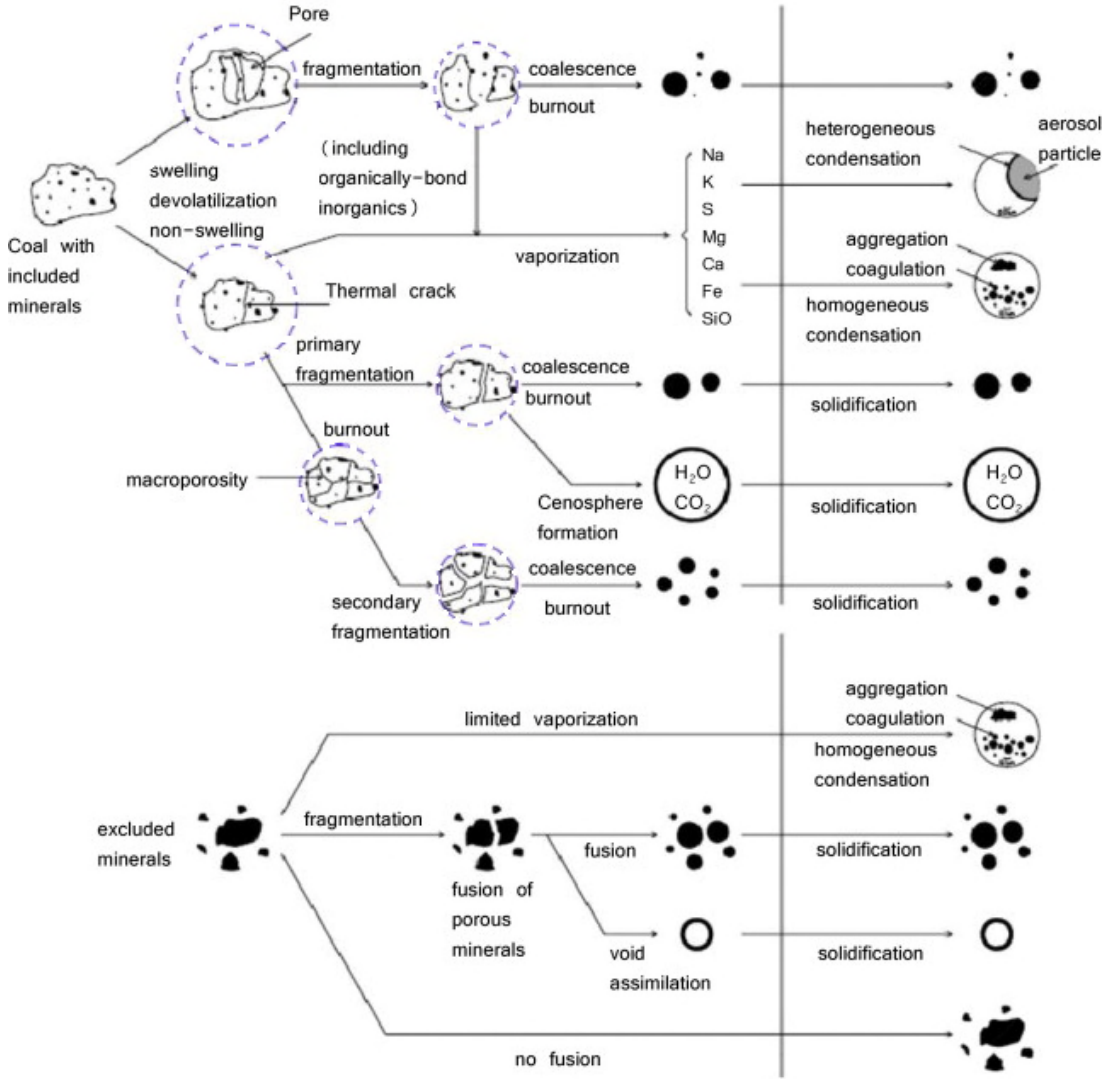

Figure 25: Ash formation mechanisms during coal combustion; the dotted line circles indicate reducing atmospheres (adapted from [195])

Effect of coal properties. It has been reported that higher rates of char fragmentation resulted in smaller fly ash particle size [196]. Tang et al. [197] reported that vitrinite particles (with higher H:C) produced highly porous char with severe fragmentation during combustion, which in turn, resulted in formation of fine ash. According to Buhre et al. [198], most of the evaporated water-soluble inorganic matter (mostly present in low rank coals or black liquor) and organically-associated inorganic matter contributed to the formation of PM1. In addition, experiments on the effects of alkalis[199-201] and sulfur [202, 203] in raw coals were conducted in drop-tube furnace to study the formation of PM1. Higher alkalis and sulfur content were expected to improve the

amount of PM1, especially particles under 0.6μm. Char produced by different types of coal may also have caused particle size distribution differences [204]. The experiments of Attalla et al. [195] showed that, compared to lignite, much more extensive fragmentation took place in bituminous coals, resulting in a narrower size distribution of particles. In addition, the particle size of coal char showed a greater influence on fragmentation in bituminous coals [195].

Effect of residence time. It is also possible that some larger mineral particles may be only partly melted due to the short residence time in the boiler, forming fly ash particles with non-spherical shapes. When the load is reduced, the temperature and flue gas flow rate in the boiler decrease accordingly. As a result, the residence time of particles is extended. It seems reasonable to expect that with longer particle residence time, more melting will occur in pulverized coal boilers. In that case, the vaporization proportion of fly ash aerosols would increase to some extent and enhance the concentration of fine particulate matter in the fly ash. In addition, the physical properties of mineral particles can be expected to affect the particle size distribution. Mineral particles with relatively high melting points could leave the pulverized coal boiler without entering the vapor phase. Moreover, non-volatile species may appear in the vapor phase due to association with organic material, and some volatile elements may be trapped within the liquid matrix material [196].

Effect of combustion environment. Combustion environment and flame temperature have already been shown to affect fine-ash formation. A reducing and high-temperature environment caused evaporation of inorganic matter, including both trace and major elements from the coal matrix [205]. Also, a CO_2-rich environment has been shown to reduce the fragmentation of carbonate minerals. As mentioned in Section 4.2, higher char particle temperatures during the combustion or gasification of coal may cause higher vaporization of inorganic matter and thus enhanced concentration of fine particles.

In general, it can be expected that with a higher rate of char fragmentation, longer residence time, and higher flame temperature, a larger proportion of fine particles will be generated, which will enhance the enrichment of arsenic in fly ash.

4.4.2 Arsenic partitioning pathway

Senior et al. [206] pointed out that the transformation of arsenic in coal to ash was actually the process of arsenic migrating into the different size fractions of ash, namely arsenic partitioning, based on the formation and deposition of fine particles.

Ratafia-Brown [147] identified five physical-chemical processes that controlled trace element partitioning and determined their final physical form, namely: heterogeneous condensation on the existing fly ash particles and heat exchange surfaces (Pathway 1); homogeneous condensation (nucleation) and coalescence as submicron aerosols if local supersaturating conditions exist (Pathway 2); physical/chemical adsorption on fly ash particles (Pathway 3); homogeneous and heterogeneous chemical reaction among trace elements, fly ash, and flue gas constituents (Pathway 4); remaining in the vapor phase for species with high vapor pressure at typical boiler exit temperature (Pathway 5).

All the pathways except Pathway 5 are volatility-dependent, supporting the hypothesis that the volatilization process provides the critical input for the transformation of arsenic.

4.5 Partitioning model

Thermodynamic equilibrium calculations, which consider coal as a homogenous material, have been widely used to predict the transformation of arsenic compounds in coal [72, 76, 207-210]. Although various factors have been considered, such as temperature, pressure, atmosphere, and other interactions, the calculation results are

thermodynamic ones; they do not account for the reaction kinetics and heterogeneous nature of coal [76]. In the early 1990's, Linak and Wendt [211, 212] began to place emphasis on prediction of the size-segregated distribution of trace metals in power plants. It was found that the partitioning of trace elements on sized fly ash was controlled by fuel composition and combustion conditions. Subsequently, the nucleation, film condensation, and coagulation processes that govern the particle size distribution of multiple toxic metals in practical combustion environments were experimentally and theoretically explored by Davis et al. [213]. The size-fractionated fine particles were shown to be in good agreement with aerosol dynamics theory. Helble [169] developed a model of trace element emissions with the input data of fundamental laboratory results on trace element partitioning. The model indicated that with element incorporation and size-dependent partitioning and penetration, the predicted arsenic concentration in flue gas could be improved by more than 25%. Subsequently, Senior el al. [61] developed a one-dimensional model to predict the behavior of arsenic in the post-combustion region as a function of gas residence time. Heterogeneous condensation and surface reaction of arsenic on fly ash as well as the effect of SO_2 on arsenic partitioning were considered in the model. The model assumed that the particle size distribution of fly ash did not change with temperature and time. More recently, James et al. [214] developed a computational fluid dynamics model of arsenic partitioning. Previously developed mathematical approaches, combined with pyritic mineral transformation mechanisms, excluding fragmentation, and recently determined experimental speciation details, were employed to predict trace element partitioning and spatial evolution during combustion. However, they only considered the particle size distribution of fly ash, and not the interaction and impact of arsenic and other elements. In future, more effort is required to develop a model of arsenic partitioning in which the particle size distribution of fly ash with gas residence time, the heterogenous/homogeneous condensation of arsenic, and the reactions between arsenic and other species could

all be included.

Zeng et al. [215] established the first quantitative physicochemical model for vaporization of arsenic during coal pyrolysis and combustion. The vaporization process for arsenic consists of three consecutive processes: transport of molecules or atoms through the bulk pyrite liquid (melt) to the melt/gas interface, vaporization of arsenic on the surface of melts, and transport of molecules/atoms through the pores of the char to the atmosphere. The controlling step is diffusion through the melt. Raeva et al. [216] presented a new method for the direct measurement of kinetic parameters under conditions that simulated the vaporization of inorganic material during coal combustion. This method was used to generate key physical property data which were necessary for modeling and assessment of the vaporization behavior of trace elements.

However, the model of arsenic volatilization is far from well-developed and trace elements may be in the form of organically associated material (incorporated into the organic structure of the coal), inclusions, or exclusions [217, 218]. The volatilization characteristics of arsenic in various forms are significantly different. For example, arsenic in the exclusion form is easily released into the atmosphere with the combustion of coal, while arsenic which is organically associated with coal is always going to be released by devolatilization, particle fragmentation, char combustion, and burnout. Because char simultaneously reacts with the oxygen in the surrounding environment, vaporization of arsenic that is organically associated with coal may occur mainly in a reducing atmosphere, as shown in Fig. 25 (represented by dotted line circles). That is to say, arsenic in different forms shows different volatilization characteristics along with the combustion of coal particles. However, the current models of arsenic volatilization do not separate organic-, inclusive-, and exclusive-related arsenic forms. These models typically assume a uniform dispersion of inclusive-related material within the char particle [219]. One reason for this is that it is not physically possible to utilize real coal particles to generate data for these three

forms separately. In addition, the model results for volatilization of arsenic under micro-environmental conditions cannot be confirmed in actual furnace combustion experiments. The arsenic volatilization model requires further improvement to establish the partitioning behavior of arsenic.

5 Emission of arsenic in coal-fired power plants

5.1 Collaborative control of arsenic by ESP and FGD equipment

The application of air pollution control devices (APCDs) in power plants can significantly affect the redistribution of arsenic in combustion by-products and alter the route by which the elements reach the environment [220]. A certain proportion of trace elements can be partitioned into the solid by-product (gypsum) and water stream (e.g. gypsum slurry) after passing through flue gas desulfurization systems [221]. Particulate-bound metals can be captured by particulate control facilities such as ESPs and fabric filters. Fly ash captured by ESP is used as a raw material for the synthesis of construction material such as cement and concrete because of its pozzolanic properties [222]. However, the fact that arsenic is largely enriched in fly ash should not be ignored. In addition, under more restrictive environmental regulations, most coal power stations are equipped with FGD systems, which could control acid gas emissions and also effectively control gaseous and particulate arsenic emissions [123]. FGD gypsum with arsenic can be used in wallboard manufacture, or for some applications as a lime substitute [223]. FGD gypsum is also employed as a landfill material in mine reclamation [224]. Some fly ash and FGD gypsum end up in landfill. Although FGD gypsum is regarded as environmentally friendly at present, it could become an issue with increasing landfill closures if further uses are not found for it [70]. Because of the wide use of fly ash and FGD gypsum, as well as the fact that they may be arsenic carriers, a better understanding is needed of the effects of APCDs on arsenic emissions.

5.1.1 Effect of ESP

The enrichment of arsenic on fine fly ash has been summarized in Section 4.2. However, researchers have reached varying conclusions on gaseous arsenic removal efficiency using ESP. For example, the study of Cheng et al. [156] on the partitioning of several trace elements in a full-scale coal combustion process in China showed that the removal efficiency of arsenic by an ESP unit was as high as 97%. But, according to Tang et al. [70], the average removal efficiency for arsenic was 83%, based on an investigation of two pulverized coal-fired power plants in China that burned bituminous coal. An ESP removes trace elements presented in the form of PM, but removal efficiencies depend on the efficiency of the ESP and the mineral content of the fly ash.

In recent years, a new dust control technology called electrostatic- fabric- integrated precipitator (EFIP) has become increasingly common. This technology combines the advantages of ESP and the bag filler, and is believed to be a low cost, promising, high efficiency for fine particle removal. Wang et al.[225] carried out a full-scale field investigation on trace element emission at a power plant equipped with EFIP. The study of field sampling results showed that the arsenic concentration contained in electrostatic precipitation ash was larger than that in the fabric filtration ash. Also, the arsenic contained in fabric filtration ash tended to release into the environment more easily.

5.1.2 Effect of FGD

Trace elements in the FGD system come mainly from limestone, flue gas, and PM, as well as the slurry water. Córdoba et al. [158] studied the abatement capacity of trace elements (including arsenic) in a large pulverized coal combustion power station equipped with a wet limestone flue gas desulfurization unit (WFGD), concluding that the control rate of arsenic (moderately volatile element) was more than 92% [158]. Similarly, Álvarez-Ayuso et al. [224, 226] conducted sampling experiments in a coal-fired power plant, which consisted of feed coal, boiler slag, fly ash, limestone, FGD gypsum, process water, and waste water. Data analysis showed

that arsenic entering the FGD system was mainly in the gaseous form, which was not consistent with the view of Córdoba et al [158]. A possible reason is that the arsenic content of the limestone feed was relatively high in the experiment of Córdoba et al., while arsenic content of the limestone was 1 mg/kg in the work of Álvarez-Ayuso et al. [224].

WFGD is considered to have high collection efficiency for gaseous arsenic. Córdoba et al. [158] considered that a large part of the arsenic (90%) was absorbed by the gypsum slurry, while the arsenic discharged from the WFGD system was in the form of PM (6.6%) and a small portion of arsenic-bearing species was emitted in gaseous form. Álvarez-Ayuso et al. [224] also concluded that WFGD systems had a high trapping ability for arsenic with 96% to 100% of the gaseous arsenic trapped by the WFGD system. Meij [120] found a trapping ability of 75%. Using on-site sampling data, Tang et al. [70] calculated a trapping ability of only 61% and suggested that there was no relationship between operating conditions and removal capacity of gaseous arsenic. In FGD systems, trapped arsenic most likely combined to form calcium-arsenate. Tang et al. [70] further suggested the specific binding form was $Ca_3(AsO_4)_2$.

5.2 Total emission of arsenic in power plants

Based on arsenic content in feed coals, combustion products, and desulfurization products collected in field tests, researchers have predicted the overall arsenic emissions from power plants [70, 159]. Tang et al. [70] investigated the distribution of arsenic (including feed coal and its combustion products) in two 600-MW Chinese coal-fired power plants (the Luohe Power Plant and Pingwei Power Plant). Both were equipped with ESP and FGD systems and fed with pulverized bituminous coal from the Huainan coalfields. The bottom ash, fly ash, feed coal, limestone, FGD gypsum, and process water were collected simultaneously to calculate the total emission and stack emission proportion of arsenic. The results showed that the average removal efficiencies of

arsenic by the ESP and FGD units were 83% and 61%, respectively. The average stack emission ratio of arsenic was 6% and the total annual emissions of arsenic from the two plants were estimated at 0.46 t [70]. Quispe et al. [159] studied the changes in mobility of arsenic in coal during combustion at a power plant in Santa Catarina, Brazil. The power plant, equipped with ESP, generated 857 MW/h of electricity with a consumption of 200,000 tons of coal per month. Considering only the easily soluble fraction, they believed that coal ash could trap 1.7 t of arsenic annually. Furthermore, by taking the mobile metal fraction of the combustion ash into consideration, they estimated that the amount of arsenic which would affect the surrounding environment was 19 t per year [159].

The differing boiler capacity, feed coals, and pollution control devices among power stations could have led to large differences in the emission data of arsenic. An overall emission factor for arsenic into the atmosphere was proposed by Kang et al. [54], as shown in Table 7.

Table 7: The worldwide arsenic emission factor from coal-fired power plants in ten countries [54]

Country	Emitted via fly ash	Emission factor for arsenic to the atmosphere	Nationwide emission	Reference
Bulgaria		Maximum 30%-40%		Vassilev and Vassileva [227]
US		3.90%		Helble [169]
Spain		1.20%		Otero-Rey et al. [127]
China		2.16%		Guo et al. [155]
Japan		0.56%	0.251 t	Ito et al. [228]
Thailand	51 mg/MWh			Kuprianov [229]
Canada		0.85%		Goodarzi [50]
India		1.60%		Reddy et al. [128]

Estonia	0.68g/t coal		Häsänen et al. [230]
Worldwide	15-100μg/MJ	232-1550 t	Nriagu and Pacyna [231]

Ash disposal, like direct emissions of gaseous arsenic, can cause harm to the environment. When large amounts of fly ash were stored temporarily in stockpiles, or disposed of in ash landfills or lagoons [232], harmful elements in the fly ash migrated or leached into the surrounding soil and groundwater due to the effects of acid rain [233]. Bata et al. [234] reported that arsenic was more easily leachable than the other heavy metals in fly ash. However, Otero-Rey et al. [235] concluded that leachable arsenic was less than 20% of total arsenic in fly ash. Effective controls on toxic elements such as arsenic are therefore recommended before fly ash, gypsum, etc., are used as building materials.

5.2.1 Emission of arsenic in China

Tian et al.[236] studied the atmospheric emissions of arsenic in China from 2002 to 2010 by combining the detailed coal consumption data, element content in coal, and the specific emission factors which were classified by different boiler patterns and APCD configurations. The emission of arsenic from coal-fired power plants in China is shown in Figure 26.

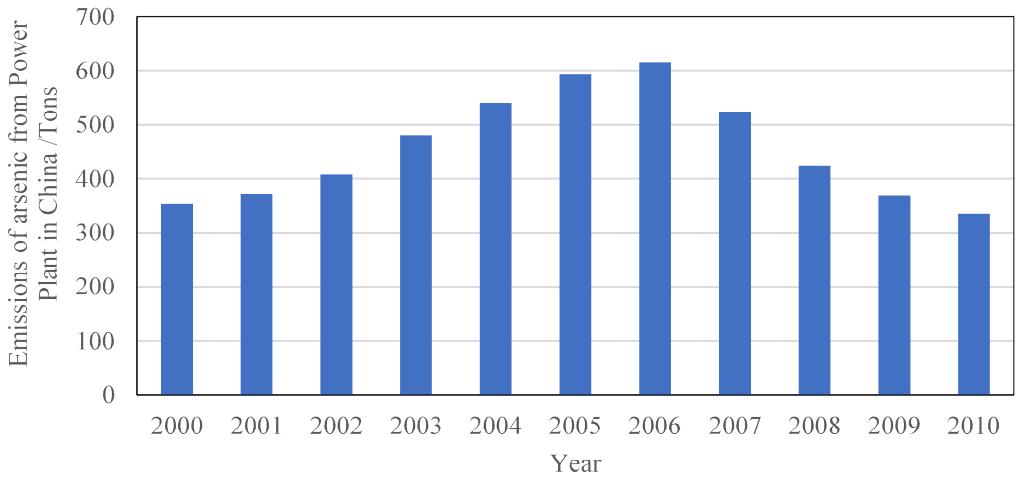

Figure 26: Emission of arsenic from coal-fired power plants in China, 2000-2010, data from [236]

As seen in Figure 26, the atmospheric emissions of arsenic from coal combustion in China increased from

354.01 t in 2000 (based on 545.9 Mt coal used) to 615.70 t in 2006 (based on 1527 Mt coal used), and then decreased gradually to 335.45 t in 2010 (based on 1591.0 Mt coal use). This decline can be mainly attributed to the installation of APCD systems. With advanced high-efficiency-control-technology and specialized mercury-control technology, the total amount of arsenic emitted in China was expected to decline to 215.57 t in 2020 [236].

6 Arsenic removal technologies

Power plants face enormous challenges in respect of arsenic emission control [71]. The existing particulate control devices, such as ESP and fabric filters, are not very efficient in controlling emissions of arsenic attached to submicron PM, let alone the arsenic in the vapor phase. Several control options are discussed below.

6.1 Removal of arsenic by calcium-based sorbents

Because of their availability and low cost, calcium-based sorbents are widely used for SO_2 and CO_2 capture and many researchers have explored the adsorption properties of calcium-based sorbents, mainly CaO, $Ca(OH)_2$, $2CaO{\cdot}SiO_2$, and $CaO{\cdot}SiO_2$ for gaseous arsenic retention [71, 80, 81, 237, 238]. Due to differences in the specific surface area of calcium-based materials, reported concentrations of gaseous arsenic and adsorption time vary considerably among different studies and specific values of adsorption experiments (adsorption efficiency, amount of arsenic captured, etc.) are difficult to compare. Therefore, only adsorption trends are considered here.

6.1.1 Effect of temperature

Temperature is an important parameter in evaluating arsenic adsorption properties of sorbents. Currently, the focus is on the medium- and high-temperature range (400-1000ºC) under an oxidizing atmosphere. However, there is still no unanimous conclusion about the impact of temperature and the resulting adsorption product at

different temperatures.

Some researchers have suggested that for calcium-based adsorbents temperature has a positive effect on arsenic adsorption [69, 80, 237]. At 400-1000ºC, Mahuli et al. [237] found that temperature could facilitate arsenic adsorption despite the surface sintering caused by the elevated temperature. Their research indicated that the adsorption efficiency of a low-surface-area sorbent in high temperatures could exceed that of a sorbent with high surface area functioning at relatively low temperatures. Researchers from Tsinghua University carried out experiments on arsenic adsorption over CaO at 400-1000ºC [80]. Their conclusions were similar; however, the focus of their studies was on the initial reaction rate of CaO and As_2O_3. The experimental results of Sterling and Helbe [69] also indicated that increased temperature could promote arsenic adsorption over CaO. Chemical adsorption is believed to be the main process between gaseous arsenic and calcium-based adsorbent in the medium- to high-temperature interval. To verify the adsorption type, Mahuli et al. [237] placed the post-sorption samples under nitrogen atmosphere at 800ºC and 1000ºC for desorption. They found that arsenic content in the samples was almost the same before and after desorption. This effectively irreversible capture reaction indicated that chemical adsorption was dominant in the process. With respect to the adsorption product, the above researchers have suggested that the post-sorption sample of calcium-based adsorbent was $Ca_3(AsO_4)_2$ (or $Ca_3As_2O_8$).

Other researchers have suggested that increased temperature enhanced the arsenic adsorption ability of calcium-based adsorbent within a certain temperature range. However, adsorption capacity decreased if the temperature exceeded a certain critical value. Jadhav et al. [71] studied the adsorption properties of gaseous arsenic over CaO at 300-900ºC. The results showed that as the temperature increased, the adsorption capacity increased between 300ºC and 600ºC and then decreased. Related research from Chen et al. [81] presented similar

results, and showed that temperature had positive effects on the arsenic adsorption capacity of CaO from 300-500ºC, but negative effects from 500-1050ºC. However, the findings of both groups present some problems in terms of distinguishing post-sorption samples. Jadhav et al.[71] have suggested that the reaction product of calcium oxide with arsenic was $Ca_3As_2O_8$ at 300-600ºC and $Ca_2As_2O_7$ at 700-900ºC. $Ca_2As_2O_7$ has thermal instability, which is the main reason that arsenic adsorption capacity decreased at higher temperatures. The reaction equations are as follows[71]:

Below 600ºC:

$$As_2O_3(s) \leftrightarrow \frac{1}{2}As_4O_6(g) \quad \text{(Eq.1)}$$

$$3CaO(s) + \frac{1}{2}As_4O_6(g) + O_2(g) \rightarrow Ca_3As_2O_8(s) \quad \text{(Eq.2)}$$

Between 700ºC and 900ºC:

$$As_2O_3(s) \leftrightarrow \frac{1}{2}As_4O_6(g) \quad \text{(Eq.3)}$$

$$2CaO(s) + \frac{1}{2}As_4O_6(g) + O_2(g) \rightarrow Ca_2As_2O_7(s) \quad \text{(Eq.4)}$$

In the view of Chen et al. [81], the reaction product of CaO with arsenic was $Ca_3(AsO_4)_2$ at all temperatures and the main reason that the adsorption capacity of CaO on arsenic decreased from 500ºC to 1050ºC was because $Ca_3(AsO_4)_2$ generated under different temperatures had different crystal phases. Compared with the low-temperature range, the adsorption product $Ca_3(AsO_4)_2$ in the high-temperature range was less thermally stable, and the decomposition of $Ca_3(AsO_4)_2$ at 500-1050ºC led to the reduced adsorption capacity of CaO. In the recent work of Zhang et al. [75], the conclusions of Chen et al. [81] were partially validated. Furthermore, through thermodynamic simulation, Zhang et al. [75] found that the adsorption process (described as Eq.2) was an exothermic reaction which could explain the temperature impact on arsenic.

The adsorption procedures for arsenic in a majority of these experiments were similar, where solid As_2O_3 was adopted as the arsenic source while the adsorption experiments were carried out in a secondary fixed bed

reactor. However, the experimental results were not identical. There are many reasons for this, the most important of which probably lies in the extremely low arsenic concentrations used in these experiments. In addition, online detection of gas-phase arsenic is not possible at present and experimental error easily occurs during off-line detection. What should be noted is that all researchers mentioned here believe chemical adsorption is the dominant process in the medium- to high-temperature interval in oxidizing condition, which is an important characteristic of arsenic adsorption over calcium-based sorbents.

6.1.2 Effect of SO_2

Some researchers have explored the effect of SO_2 on the arsenic adsorption process of calcium-based sorbents. However, there is no agreement on SO_2 impact to date. Li et al. [80] made an exhaustive study of simultaneous adsorption of SO_2 and As_2O_3 vapor and showed that SO_2 did not have a significant impact on arsenic adsorption. Two main factors could explain this. First, the reaction rate constant of CaO with gaseous arsenic is greater than that of the desulfurization reaction, which means SO_2 does not compete with As_2O_3 active sites on the surface of CaO at the initial stage of the reaction. Second, they demonstrated that calcium sulfate also has the ability to adsorb gaseous arsenic. Therefore, even if the CaO surface was completely sulfated, it would still show some gaseous arsenic adsorption capacity.

Chen et al. [81] recently investigated the effect of SO_2 on the arsenic adsorption process of calcium-based sorbent over a wide temperature range (300-1050ºC). The results showed that SO_2 could partially inhibit the arsenic adsorption process at 300-800ºC and at 800ºC the adsorption suppression was the most pronounced. However, as temperature increased further, the inhibitory effect of SO_2 weakened. At 1050ºC a promotional effect of SO_2 on arsenic adsorption was observed. They attributed that to SO_2 competing with gaseous As_2O_3 for adsorption sites and the sulfation product $CaSO_4$ occupying the active sites, weakening arsenic adsorption. The

sulfation product may be expected to further block surface pore structure of the sorbent resulting in surface area decrease, which would further restrict arsenic adsorption by CaO. As to the promotional effect of SO_2 in the high-temperature range, they agreed with Li et al. [80] that $CaSO_4$ also had arsenic adsorption capacity.

The common conclusion is that $CaSO_4$ arsenic adsorption capacity must be considered. However, there is no unified conclusion about the SO_2 impact and further studies are needed.

6.1.3 Kinetic studies

To better understand the arsenic adsorption process of calcium-based sorbents, researchers have carried out kinetic studies. In 1997, a kinetic equation describing the reaction between CaO and As_2O_3 was put forward by Mahuli et al. [237]. The reaction can be described as:

$$\frac{dx}{dt} = -k_s C_g^m A_{CaO}^n \quad \text{(Eq.5)}$$

where x is the overall conversion ratio of CaO; Cg is the concentration of the gaseous As_2O_3; m is the reaction order with respect to the gaseous species; n is the reaction order based on sorbent surface area; A_{CaO} is the specific surface area of the sorbent; k_s is the reaction rate constant; and t is the reaction time. They assumed n = 1 and used the equation $A_{CaO} = S_0(1-x)$ to describe sorbent surface area. Thus, the above equation could be described as follows:

$$\ln\frac{1}{1-x} = k_s C_g^m S_0 t \quad \text{(Eq.6)}$$

By taking the natural logarithm of both sides of Eq.6 and obtaining the relationship between ln(-ln(1-x)) and lnC_g, $m\approx1$ was calculated. In this case, the assumption of $n\approx1$ was verified. The apparent activation energy of the adsorption reaction was 43.9 kJ/mol. However, there were no specifics concerning frequency factor.

Other researchers have carried out kinetic studies of the reaction between CaO and As_2O_3 based on the research of Mahuli et al. [237] These results are summarized in Table 8.

Table 8: Comparison of specific rate constant for surface-reaction-controlled gas-solid reactions

Gas-solid reaction	Frequency factor	Activation energy	Temperature	Over all reaction order	Reference
$CaO+As_2O_3$		43.9 kJ/mol	600ºC	n=1	Mahuli et al. [237]
$CaO+As_2O_3$	1.4 mm/s	23 kJ/mol	600-1000ºC	n=1	
$2CaO·SiO_2+As_2O_3$	7.2 mm/s	28 kJ/mol	600-1000ºC	n=1	Sterling and Helble [69]
$CaO·SiO_2+As_2O_3$	5.5 mm/s	30 kJ/mol	600-1000ºC	n=1	
$CaO+As_2O_3$			600-900ºC	n=0.86	Li et al. [80]
$CaO+As_2O_3$	0.9 mm/s	25.99 kJ/mol	600-900ºC	n=1.1	Zhang et al. [75]

Jadhav et al. [71] proposed a novel shrinking core mechanism model to describe the reaction between CaO and As_2O_3. In this model, the specific surface area and pore size were 3.2 m^2/g and near 0 cm^3/g respectively, which were assumed to be low enough to ensure negligible mass transfer resistance. The conversion ratio of CaO can be expressed as follows,

$$(3k\,C_g^n/\rho_m)(1/r_p)t = 1-(1-x)^{1/3} \quad \text{(Eq.7)}$$

where x is the overall conversion ratio of CaO; r_p is particle radius of CaO; ρ_m is the density of CaO; k is the reaction rate constant; C_g is the concentration of the gaseous arsenic; t is the reaction time; and n is the order of Eq.7. To eliminate the mass transfer resistance, a higher gas velocity (≈0.4 m/s) and smaller solid sorbent particles (<2 μm) were used in the adsorption experiments. Jadhav et al.[71] studied the effect of gaseous arsenic concentration as well as adsorption temperature on CaO conversion rates. By combining the Arrhenius equation with Eq.7, they obtained activation energy of 21.34 kJ/mol and the order of reaction with respect to arsenic concentration (n) was close to 1. They suggested that such low activation energy indicated the reaction had a slow temperature response. It is noteworthy that the reaction time was controlled in less than 10 min in these

experiments, which eliminated the effect of diffusion of ionic species (Ca^{2+} and O^{2-}) through the product layer. Thus, the activation energy they calculated was lower than that of Mahuli et al. [237].

Kinetic study of the adsorption reaction depends on experimental data and the kinetic model. Kinetic parameters could be signficantly different because different kinetic equations were adopted and different experimental parameters were applied. However, the reaction order with respect to arsenic concentration is close to 1, which appears to be a common conclusion [69, 71, 75, 80, 237].

6.2 Removal of arsenic by metal oxide sorbents

In order to explore more efficient arsenic sorbents, Zhang et al. [75] studied gaseous arsenic adsorption on three metal oxides (Fe_2O_3, CaO, and Al_2O_3). In Figure 27 experimental data at 600-900ºC show that Fe_2O_3 had a greater adsorption capacity under the same experimental conditions.

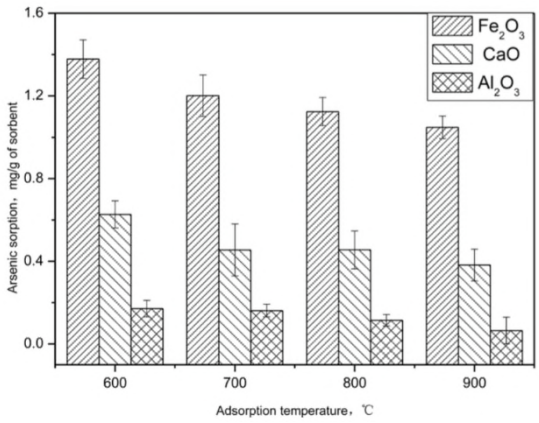

Figure 27: Amount of arsenic captured by various metal oxide adsorbents at different temperatures[75]

Adsorption capacity of sorbents increased in the following order: Al_2O_3 < CaO < Fe_2O_3 at 600-900ºC. Compared with CaO and Fe_2O_3, Al_2O_3 had a larger specific surface area. But adsorption capacity of Al_2O_3 was the lowest. What is more, the thermal desorption experiment of post-sorption samples showed that little arsenic loss was observed in CaO and Fe_2O_3. However, the arsenic content in the post-sorption sample of Al_2O_3 was

only 2.21% of the original content. Zhang et al. [75] inferred from this that physical adsorption was the main process of arsenic adsorption on Al_2O_3. Their XRD results also confirmed this conclusion, showing As_2O_3 was detected on the Al_2O_3 surface. They calculated and compared kinetic parameters of CaO and Fe_2O_3 for arsenic adsorption, as shown in Table 9.

Table 9: Specific rate constant for surface reaction of sorbents CaO and Fe_2O_3 [69]

reactant	reaction order	activation energy, kJ/mol	frequency factor, s^{-1}
CaO	0.8	25.99	0.009
Fe_2O_3	1.1	12.17	0.034

Similarly to the work of Jadhav et al. [71], Zhang et al. [75] suggested that the adsorption process was slow in response to temperature change by comparing the kinetic parameters of CaO and Fe_2O_3. They proposed that the frequency factor could describe active site quantities on the sorbent surface, in which adsorption would take place.

Subsequently, Zhang et al. [239] developed an iron-based sorbent Fe_2O_3/γ-Al_2O_3 for gas-phase arsenic capture, on the basis of their preliminary study. They identified the optimum operating temperature as being around 600ºC, by carrying out adsorption experiments at 150-900ºC. SO_2 was considered to have a promotional effect on arsenic adsorption, whereas, NO was believed to have little impact. They suggested that SO_2 would be oxidized by Fe^{3+} on the sorbent surface, generating SO_4^{2-} and HSO_4^-, which could facilitate the oxidation of As^{3+} to As^{5+}. And then, As^{5+} reacted with Fe_2O_3, which was the active ingredient of the sorbent, forming $FeAsO_4$.

The catalytic oxidation effect of iron-based sorbents may play a significant role in the adsorption process. However, an accurate description of the valence changes of the iron ions as well as the reaction mechanism for the lattice oxygen are lacking in the available literature.

In addition, Rupp et al.[240] proved that the Pd/γ-Al_2O_3 had the ability to remove AsH_3 from a simulated fuel gas under laboratory conditions. With a sorbent bed containing ten pounds of Pd/γ-Al_2O_3 held at 260℃, nearly 100% of selenium, arsenic and mercury within a dirty fuel gas slipstream were removed. The results indicated that arsine, phosphine and hydrogen selenide competed against each other for sorption sites. However, the performance of Pd/γ-Al_2O_3 on $As2O_3$(g) removal is still unclear.

6.3 Removal of arsenic by fly ash sorbents

A significant proportion of the gaseous arsenic in flue gas migrates into fly ash due to a condensation or reaction process during coal combustion [241]. This means that fly ash could be used as sorbent material for trace element removal. To explore the adsorption capacity of fly ash on arsenic, López-Antón MA et al. [187] carried out a series of adsorption experiments in a fixed-bed reactor. Two fly ash samples were selected as sorbents. One sample was taken from a fluidized bed combustion plant burning a mixture of coal wastes and the other was taken from a pulverized coal power plant burning high-rank coals. Adsorption experiments at 120ºC showed that maximum retention capacity of fly ash for gaseous arsenic was 5.3 mg/g and the corresponding maximum adsorption efficiency was less than 20%. Díaz-Somoano et al. [73] estimated that calcium and iron in fly ash played a key role in arsenic adsorption by measuring the content of calcium, iron and arsenic.

Díaz-Somoano et al. [73] investigated gaseous arsenic adsorption by fly ash at 120ºC, a relatively low temperature. This was because high temperatures may cause re-carbonization of the unburned carbon in fly ash, resulting in changes to fly ash sorbents. In addition, while 120ºC was close to the temperature at the inlet of ESP, which was convenient for fly ash sorbent injection, gaseous arsenic was prone to condense on the tube wall at 120ºC, increasing the likelihood that such laboratory scale adsorption experiments would produce significant errors.

6.4 Removal of arsenic by carbon-based sorbents

As early as 1979, Wouterlood and Bowling [242] explored the possibility of using activated carbon in gaseous arsenic removal. They found that the selected activated carbons could adsorb 25% to 45% of arsenic at 200ºC when the concentration of arsenic was 14.64-20.24 mg/L. The breakthrough time was more than 10 h (10.75-17.5 h). Comparing the adsorption performance of four kinds of activated carbon, it was found that the adsorption of arsenic increased with the specific surface area of the sorbent, however not in a linear fashion. They also found that As_4O_6 could be efficiently desorbed by heating the adsorbent in a non-oxidizing gas. Even after many adsorption-desorption reaction cycles, the arsenic adsorption performance did not change appreciably (14 cycles).

Subsequently, López-Antón et al. [238] conducted arsenic adsorption experiments over activated carbon at 250ºC in an arsenic concentration of 0.4 μg/mL. They found the behavior of activated carbons in arsenic retention did not appear to be dependent on the porous texture of activated carbon, by comparing the adsorption performance of different pore structures of activated carbon. The metal elements in the activated carbon, such as calcium and iron, played a catalytic role in arsenic adsorption. Although sulfur in activated carbon will affect the adsorption of mercury, they suggested that the sulfur content in the activated carbon would not cause any impact on arsenic adsorption.

In summary, there are three main reasons for arsenic adsorption by activated carbon. First, the large specific surface area and abundant pore structure of activated carbon increases the possibility of physical adsorption of arsenic. Second, the metallic elements in activated carbon, such as calcium and iron, can play a catalytic role during arsenic adsorption. Third, modified commercial activated carbons may contain some haloid elements, which could facilitate arsenic adsorption. However, the raw materials and preparation processes for producing

activated carbon are vastly different, which often leads to different and even diametrically opposite conclusions [238, 242]. In general, the research on arsenic adsorption over activated carbon is still inconclusive.

6.5 Arsenic adsorption in oxy-fuel combustion flue gas

Due to the gas recirculation and the absence of nitrogen, the SO_2 concentration in the flue gas of oxy-fuel combustion is much higher than in air combustion. In addition, the H_2O vapor concentration in oxy combustion is particularly high. When the same kind of coal is burned, it is reported that the water vapor concentrations in air combustion and oxy-fuel combustion are 10% and 31%, respectively [243]. Wang et al. [244] explored the arsenic adsorption characteristic of iron-based sorbent in oxy-fuel combustion flue gas and proposed that the adsorption mechanism followed the Mars-Maessen mechanism[245]. In oxy-fuel combustion conditions, the high concentration of CO_2 had a significant adverse effect on arsenic adsorption. However, the presence of O_2 as well as H_2O(g) promoted arsenic removal in the CO_2-enriched atmosphere. The increased SO_2 concentration was proved to accelerate the adsorption process with generation of active species (HSO_4^-/SO_4^{2-}), while with the increase of SO_2 concentration in flue gas, the competition between SO_2 and arsenic on iron-based sorbents adsorption was strengthened.

7 Conclusions

Coal combustion is one of the main anthropogenic sources of arsenic pollution in the environment. Due to its high toxicity, volatility, and potentially carcinogenic properties this element is receiving increasing attention. This paper summarized the properties of arsenic in coal, the factors affecting arsenic volatilization during coal combustion, the transformation behavior, mechanism and model of arsenic in post-combustion processing, and the emission and removal technologies of arsenic in power plants.

Temperature has a positive effect on both the volatilization rate and the degree of volatilization, and temperature-staged volatilization characteristics of arsenic. Differences in the mode of occurrence of arsenic in coals could result in different volatilization proportions of arsenic even at the same temperature. It is generally accepted that exchangeable and organic-bound arsenic are easily vaporized at the devolatilization stage of coal, while arsenic bound to iron-manganese oxides and pyrite is unstable and tends to vaporize below 1000ºC. By contrast, arsenates are very stable and usually decompose at relatively high temperatures. This indicates that coals with a large proportion of unstable arsenic compounds will have a higher degree of volatilization. As far as coal rank is concerned, no obvious correlation between arsenic volatility and coal rank has been found. In addition, while they have rarely been reported, the effects of heating rate and particle size on arsenic volatilization should be taken into consideration. Calcium, iron, magnesium, sodium and potassium tend to react with arsenic to form stable arsenates, which inhibit the volatilization of arsenic, while aluminum and silicon may have a positive effect on the volatilization behavior of arsenic. However, the related reactions and substances were based on thermodynamic analysis without considering the chemical kinetics. Simultaneous release of sulfur and arsenic were found in isothermal coal combustion, demonstrating that arsenic was closely related to sulfur in coal. The role of chlorine was also examined. Simulation results show that higher chlorine content in coal may promote the generation of more volatile compounds like $AsCl_3(g)$, which in turn increase the volatilization ratio of arsenic.

Oxy-fuel combustion is a promising and advanced technology for carbon capture. Few reports discussed the effect of CO_2 on arsenic volatilization during oxy-fuel combustion, and firm conclusions cannot be drawn. On one hand, higher CO_2 content helps to generate a reducing atmosphere in the char particle neighborhood, which could reduce arsenic oxides to more volatile sub-oxides and make the volatilization of arsenic easier. On the

other hand, higher CO_2 content inhibits mass and heat transfer, which may decrease the flame temperature and in turn have a negative effect on arsenic volatility. To date very few experiments have been carried out on the effect of SO_2 and $H_2O(g)$ on arsenic volatility under oxy-fuel conditions.

When flue gas cools in the post combustion process, vaporized arsenic species gradually transform to solid-phase and redistribute in bottom ash, fly ash and flue gas. The mass balance of arsenic from most studies is less than 100%, mainly due to the condensation or absorption of arsenic on the interior surfaces of equipment in power plants. With the application of XANES and EXAFS spectroscopy, the speciation of arsenic in feed coal and combustion products was studied. The general view is that arsenic in fly ash is mainly present in the less toxic As^{5+} form, while the speciation of arsenic in flue gas needs to be further examined. In addition, it is widely reported that most arsenic is captured by fly ash, especially ultrafine ash particles. With higher rates of char fragmentation, longer residence times and higher flame temperatures, more fine particles are expected to be generated, which in turn may enhance the enrichment of arsenic in fly ash. The enrichment of arsenic on fine particles is also affected by the sulfur content and mineral composition in the coal, and the way the combustion system is operated. Based on the close relationship between arsenic and ash particle formation, several arsenic partitioning models considering the particle size distribution of fly ash have been developed.

The application of APCDs can significantly affect the redistribution of arsenic in combustion by-products and alter the route by which the elements reach the environment. ESPs remove trace elements present in the form of PM, but not gaseous trace elements. FGD is believed to have high collection efficiency for gaseous arsenic. However, the arsenic discharged from WFGD systems is mostly in the form of PM and a small portion of arsenic-bearing species is emitted in the gaseous form.

Researchers have explored the adsorption properties of calcium-based adsorbent, metal oxides, activated

carbon and fly ash for gaseous arsenic. Calcium-based sorbents have been widely investigated due to their low cost and ready availability. The adsorption processes of these sorbents are believed to be a combination of chemical and physical adsorption. The temperature effect on arsenic removal is complicated and there is no generally supported conclusion. Research suggests that $CaSO_4$ has significant arsenic adsorption capacity and kinetic studies show that the activation energy of the reaction between CaO and As_2O_3 lies between 20-30 kJ/mol. Most researchers have suggested that the overall reaction order is 1, while values of 0.86 and 1.1 were found in two studies.

8 Acknowledgements

This work has been financed by National Key R&D Program of China (2016YFB0600701). Special thanks also go to David Granatstein for numerous editorial and technical suggestions on the manuscript.

References

[1] Environmental Protection Agency. Locating and estimating air emissions from sources of arsenic and arsenic compounds. Final report. 1998.

[2] Duan L, Li X, Jiang Y, Lei M, Dong Z, Longhurst P. Arsenic transformation behaviour during thermal decomposition of P. vittata , an arsenic hyperaccumulator. Journal of Analytical & Applied Pyrolysis. 2017.

[3] Jiang Y, Ameh A, Lei M, Duan L, Longhurst P. Solid-gaseous phase transformation of elemental contaminants during the gasification of biomass. Science of the Total Environment. 2014;30:1993-2003.

[4] Jiang Y, Lei M, Duan L, Longhurst P. Integrating phytoremediation with biomass valorisation and critical element recovery: A UK contaminated land perspective. Biomass & Bioenergy. 2015;83:328-39.

[5] Tchounwou PB, Yedjou CG, Patlolla AK, Sutton DJ. Heavy metal toxicity and the environment: Springer Basel; 2012.

[6] Smith AH, Hopenhayn-Rich C, Bates MN, Goeden HM, Hertz-Picciotto I, Duggan HM, et al. Cancer risks from arsenic in drinking water. Environmental Health Perspectives. 1992;97:259-67.

[7] Kong M, Liu Q, Wang X, Ren S, Yang J, Zhao D, et al. Performance impact and poisoning mechanism of arsenic over commercial V_2O_5-WO_3/TiO_2 SCR catalyst. Catalysis Communications. 2015;72:121-6.

[8] Li M, Liu B, Wang X, Yu X, Zheng S, Du H, et al. A promising approach to recover a spent SCR catalyst: deactivation by arsenic and alkaline metals and catalyst regeneration. Chemical Engineering Journal. 2017.

[9] Peng Y, Li J, Si W, Luo J, Dai Q, Luo X, et al. Insight into deactivation of commercial SCR catalyst by arsenic: an experiment and DFT study. Environmental Science & Technology. 2014;48:13895.

[10] Environmental Protection Agency. National emission standards for hazardous air pollutants from coal- and oil-fired electric utility steam generating units and standards of performance for fossil-fuel-fired electric utility, industrial-commercial-institutional, and small industrial-commercial-institutional steam generating units. 2011.

[11] Environmental Protection Agency. National emission standards for hazardous air pollutants from coal and oil-fired electric utility steam generating units and standards of performance for fossil-fuel-fired electric utility, industrial-commercial-institutional, and small industrial-commercial-institutional steam generating units; Technical correction. 2016.

[12] Lu X, Zeng H, Xu T, Yan R. Chemometric studies of distribution of trace elements in seven Chinese coals. Fuel. 1995;74:1382-6.

[13] Querol X, Fernández-Turiel J, López-Soler A. Trace elements in coal and their behaviour during combustion in a large power station. Fuel. 1995;74:331-43.

[14] Huggins FE, Shah N, Huffman GP, Kolker A, Crowley S, Palmer CA, et al. Mode of occurrence of chromium in four US coals. Fuel Processing Technology. 2000;63:79-92.

[15] Xu M, Yan R, Zheng C, Qiao Y, Han J, Sheng C. Status of trace element emission in a coal combustion process: a review. Fuel Processing Technology. 2004;85:215-37.

[16] Luo G, Yao H, Xu M, Gupta R, Xu Z. Identifying modes of occurrence of mercury in coal by temperature programmed pyrolysis. Proceedings of the Combustion Institute. 2011;33:2763-9.

[17] Riley KW, French DH, Farrell OP, Wood RA, Huggins FE. Modes of occurrence of trace and minor elements in some Australian coals. International Journal of Coal Geology. 2012;94:214-24.

[18] Keegan T, Hong B, Thornton I, Farago M, Jakubis P, Jakubis M, et al. Assessment of environmental arsenic levels in Prievidza district. Journal of Exposure Analysis & Environmental Epidemiology. 2002;12:179-85.

[19] Kizilshtein LY, Kholodkov YI. Ecologically hazardous elements in coals of the Donets Basin. International

Journal of Coal Geology. 1999;40:189-97.

[20] Wongyai K, Garivait S, Donald O. A geochemistry study of arsenic speciation in overburden from Mae Moh Lignite Mine, Lampang, Thailand. Environmental Earth Sciences. 2010;70:2047-53.

[21] Karayigit AI, Spears DA, Booth CA. Antimony and arsenic anomalies in the coal seams from the Gokler coalfield, Gediz, Turkey. International Journal of Coal Geology. 2000;44:1-17.

[22] Mastalerz M, Drobniak A. Arsenic, cadmium, lead, and zinc in the Danville and Springfield coal members (Pennsylvanian) from Indiana. International Journal of Coal Geology. 2007;71:37-53.

[23] Ruppert LF, Hower JC, Eble CF. Arsenic-bearing pyrite and marcasite in the Fire Clay coal bed, Middle Pennsylvanian Breathitt Formation, eastern Kentucky. International Journal of Coal Geology. 2005;63:27-35.

[24] Eskenazy GM. Geochemistry of arsenic and antimony in Bulgarian coals. Chemical Geology. 1995;119:239-54.

[25] Goodarzi F, Grieve DA, Sanei H, Gentzis T, Goodarzi NN. Geochemistry of coals from the Elk Valley coalfield, British Columbia, Canada. International Journal of Coal Geology. 2009;77:246-59.

[26] Ali J, Kazi TG, Baig JA, Afridi HI, Arain MS, Ullah N, et al. Monitoring of arsenic fate with proximate parameters and elemental composition of coal from Thar coalfield, Pakistan. Journal of Geochemical Exploration. 2015;159:227-33.

[27] Pentari D, Foscolos AE, Perdikatsis V. Trace element contents in the Domeniko lignite deposit, Elassona basin, Central Greece. International Journal of Coal Geology. 2004;58:261-8.

[28] Mukherjee S, Srivastava SK. Trace elements in high-sulfur Assam coals from the makum coalfield in the northeastern region of India. Energy & Fuels. 2005;19:882-91.

[29] Luo K. Arsenic content and distribution pattern in Chinese coals. Toxicological & Environmental Chemistry. 2005;87:427-38.

[30] Ding Z, Zheng B, Long J, Belkin HE, Finkelman RB, Chen C, et al. Geological and geochemical characteristics of high arsenic coals from endemic arsenosis areas in southwestern Guizhou Province, China. Applied Geochemistry. 2001;16:1353-60.

[31] Tian HZ, Lu L, Hao JM, Gao JJ, Cheng K, Liu KY, et al. A review of key hazardous trace elements in Chinese coals: abundance, occurrence, behavior during coal combustion and their environmental impacts. Energy & Fuels. 2013;27:601-14.

[32] Yudovich YE, Ketris MP. Arsenic in coal: a review. International Journal of Coal Geology. 2005;61:141-96.

[33] Goodarzi F. Inorganic constituents of coal and their impact on coal quality. Fuel & Energy Abstracts. 1994;36:171.

[34] Chen P, Kuang H, Tang X. Research on the distribution and occurrence of arsenic in coal. Journal of China Coal Society. 2002;35:3547-.

[35] Cong FU, Bai XF, Ying J. Discussion on the relationship between the content of arsenic and the coal quality characteristic and the arsenic modes of occurrence in Chinese high arsenic coal. Meitan Xuebao/journal of the China Coal Society. 2012;37:96-102(7).

[36] Cho EH, Olajide O, Yang RYK. Two-stage coal flotation to remove pyritic sulfur, arsenic, selenium and mercury. Minerals & Metallurgical Processing. 2013;30:162-8.

[37] Cheng W, Zhang Q, Yang R, Tian Y. Occurrence modes and cleaning potential of sulfur and some trace elements in a high-sulfur coal from Pu’an coalfield, SW Guizhou, China. Environmental Earth Sciences. 2014;72:35-46.

[38] He CL, Ma SJ, Su XJ, Mo QH. Microwave roasting pyrite for removal of the sulfur and arsenic. Advanced Materials Research. 2014;881-883:1531-5.

[39] Savage KS, Tingle TN, O'Day PA, Waychunas GA, Bird DK. Arsenic speciation in pyrite and secondary weathering phases, Mother Lode Gold District, Tuolumne County, California. Applied Geochemistry. 2000;15:1219-44.

[40] Filby RH, Shah KR, Sautter CA. A study of trace element distribution in the solvent refined coal (SRC) process using neutron activation analysis. Journal of Radioanalytical Chemistry. 1977;37:693-704.

[41] Goodarzi F. Comparison of elemental distribution in fresh and weathered samples of selected coals in the Jurassic-Cretaceous Kootenay Group, British Columbia, Canada. Chemical Geology. 1987;63:21-8.

[42] Goodarzi F. Concentration of elements in lacustrine coals from zone A hat creek deposit No.1, British Columbia, Canada. International Journal of Coal Geology. 1987;8:247-68.

[43] Goodarzi F. Elemental distribution in coal seams at the Fording coal mine, British Columbia, Canada. Chemical Geology. 1988;68:129-54.

[44] Zygarlicke CJ, Steadman EN, Benson SA. Studies of transformations of inorganic constituents in a Texas lignite during combustion. Progress in Energy & Combustion Science. 1990;16:195-204.

[45] Kolker A, Chou CL. Cleat-filling calcite in Illinois Basin Coals: trace-element evidence for meteoric fluid migration in a coal basin. Journal of Geology. 1994;102:111-6.

[46] Guo R, Yang J, Liu Z. Thermal and chemical stabilities of arsenic in three Chinese coals. Fuel Processing Technology. 2004;85:903-12.

[47] Zhao R, Hu Z, Liu B. Modes of occurrence of arsenic in high-arsenic coal by extended X-ray absorption fine structure spectroscopy. Chinese Science Bulletin. 1998;43:1660-3.

[48] Kolker A, Huggins FE, Palmer CA, Shah N, Crowley SS, Huffman GP, et al. Mode of occurrence of arsenic in four US coals. Fuel Processing Technology. 2000;63:167-78.

[49] Shah P, Strezov V, Prince K, Nelson PF. Speciation of As, Cr, Se and Hg under coal fired power station conditions. Fuel. 2008;87:1859-69.

[50] Goodarzi F, Huggins FE, Sanei H. Assessment of elements, speciation of As, Cr, Ni and emitted Hg for a Canadian power plant burning bituminous coal. International Journal of Coal Geology. 2008;74:1-12.

[51] Wang M, Zheng B, Wang B, Li S, Wu D, Hu J. Arsenic concentrations in Chinese coals. Science of The Total Environment. 2006;357:96-102.

[52] Dai C, Li F. Arsenic emission characteristics during fluidized-bed coal combustion. Journal of China Coal Society. 2005;30:109-13.

[53] Zhao Y, Zhang J, Huang W, Wang Z, Li Y, Song D, et al. Arsenic emission during combustion of high arsenic coals from Southwestern Guizhou, China. Energy Conversion and Management. 2008;49:615-24.

[54] Kang Y, Liu G, Chou C-L, Wong MH, Zheng L, Ding R. Arsenic in Chinese coals: Distribution, modes of occurrence, and environmental effects. Science of The Total Environment. 2011;412:1-13.

[55] Wang J, Tomita A. A chemistry on the volatility of some trace elements during coal combustion and pyrolysis. Energy & fuels. 2003;17:954-60.

[56] Senior CL, Bool III LE, Morency JR. Laboratory study of trace element vaporization from combustion of pulverized coal. Fuel Processing Technology. 2000;63:109-24.

[57] Clarke LB. The fate of trace elements during coal combustion and gasification: an overview. Fuel. 1993;72:731-6.

[58] Bool LEI, Helble JJ. A laboratory study of the partitioning of trace elements during pulverized coal combustion. Energy & Fuels. 1995;9:880-7.

[59] Lu H, Chen H, Li W, Li B. Transformation of arsenic in Yima coal during fluidized-bed pyrolysis. Fuel. 2004;83:645-50.

[60] Liu H, Wang C, Zhang Y, Sun Z, Shao H. Effect of temperature and mode of occurrence on the migration and volatilization of arsenic during coal combustion. Journal of Chemical Industry and Engineering(China). 2015;66:4643-51.

[61] Senior CL, Lignell DO, Sarofim AF, Mehta A. Modeling arsenic partitioning in coal-fired power plants. Combustion and Flame. 2006;147:209-21.

[62] Liu H, Pan W-P, Wang C, Zhang Y. Volatilization of arsenic during coal combustion based on isothermal thermogravimetric analysis at 600–1500°C. Energy & Fuels. 2016;30:6790-8.

[63] Zeng T. Transformation of iron and trace elements during coal combustion. Boston, USA: Massachusetts Institute of Technology; 1998.

[64] Wei X, Zhang G, Cai Y, Li L, Li H. The volatilization of trace elements during oxidative pyrolysis of a coal from an endemic arsenosis area in southwest Guizhou, China. Journal of Analytical and Applied Pyrolysis. 2012;98:184-93.

[65] Shen F, Liu J, Zhang Z, Dai J. On-line analysis and kinetic behavior of arsenic release during coal combustion and pyrolysis. Environmental Science & Technology. 2015;49:13716-23.

[66] Liu H, Wang C, Zou C, Zhang Y, Wang J. Simultaneous volatilization characteristics of arsenic and sulfur during isothermal coal combustion. Fuel. 2017;203:152-61.

[67] Liu J, Zheng C, Zhang J. Study on the speciation of most volatile trace elements in Coal. Journal of Combustion Science and Technology. 2003;9:295-9.

[68] Liu S, Wang Y, Yu L, Oakey J. Volatilization of mercury, arsenic and selenium during underground coal gasification. Fuel. 2006;85:1550-8.

[69] Sterling RO, Helble JJ. Reaction of arsenic vapor species with fly ash compounds: kinetics and speciation of the reaction with calcium silicates. Chemosphere. 2003;51:1111-9.

[70] Tang Q, Liu G, Yan Z, Sun R. Distribution and fate of environmentally sensitive elements (arsenic, mercury, stibium and selenium) in coal-fired power plants at Huainan, Anhui, China. Fuel. 2012;95:334-9.

[71] Jadhav RA, Fan L-S. Capture of gas-phase arsenic oxide by lime: kinetic and mechanistic studies. Environmental Science & Technology. 2001;35:794-9.

[72] Lundholm K, Nordin A, Backman R. Trace element speciation in combustion processes-Review and compilations of thermodynamic data. Fuel Processing Technology. 2007;88:1061-70.

[73] Díaz-Somoano M, Unterberger S, Hein KRG. Prediction of trace element volatility during co-combustion processes. Fuel. 2006;85:1087-93.

[74] Seames WS, Wendt JOL. Regimes of association of arsenic and selenium during pulverized coal combustion. Proceedings of the Combustion Institute. 2007;31:2839-46.

[75] Zhang Y, Wang C, Li W, Liu H, Zhang Y, Hack P, et al. Removal of gas-phase As_2O_3 by metal oxide adsorbents: effects of experimental conditions and evaluation of adsorption mechanism. Energy & Fuels. 2015;29:6578–85.

[76] Contreras ML, Arostegui JM, Armesto L. Arsenic interactions during co-combustion processes based on thermodynamic equilibrium calculations. Fuel. 2009;88:539-46.

[77] Miller B, And DRD, Kandiyoti R. The influence of injected HCl and SO_2 on the behavior of trace elements during wood-bark combustion. Energy & Fuels. 2003;17:1382-91.

[78] Yan R, Gauthier D, Flamant G. Volatility and chemistry of trace elements in a coal combustor. Fuel. 2001;80:2217-26.

[79] Miller BB, R. Kandiyoti A, Dugwell DR. Trace element emissions from co-combustion of secondary fuels with coal: a comparison of bench-scale experimental data with predictions of a thermodynamic equilibrium model. Energy & Fuels. 2002;16:956-63.

[80] Li Y, Tong H, Zhuo Y, Li Y, Xu X. Simultaneous removal of SO_2 and trace As_2O_3 from flue gas: mechanism, kinetics study, and effect of main gases on arsenic capture. Environmental Science & Technology. 2007;41:2894-900.

[81] Chen D, Hu H, Zhang X, Liu H, Cao J, Shen J, et al. Findings of proper temperatures for arsenic capture by CaO in the simulated flue gas with and without SO_2. Chemical Engineering Journal. 2015;267:201-6.

[82] Vassilev SV, Eskenazy GM, Vassileva CG. Contents, modes of occurrence and behaviour of chlorine and bromine in combustion wastes from coal-fired power stations. Fuel. 2000;79:923-38.

[83] Akan-Etuk N, Niksa S, Kruger CH. Pyrite thermochemistry, ash agglomeration, and char fragmentation during pulverized coal combustion: Quarterly report. 1989.

[84] Srinivasachar S, Helble JJ, Boni AA. Mineral behavior during coal combustion 1. Pyrite transformations.

Progress in Energy and Combustion Science. 1990;16:281-92.

[85] Senior CL, Huggins FE, Huffman GP, Shah N, Yap N, Wendt JOL, et al. Toxic substances from coal combustion-a comprehensive assessment. Physical Sciences Inc; 2001.

[86] Zhao YC. A model for pyrite partition during coal combustion. Journal of Engineering Thermophysics. 2007.

[87] Seames WS, Jassim EI, Benson SA. Modeling trace element release from included and excluded pyrite during pulverized coal combustion. 2010.

[88] Huffman GP, Huggins FE, Shah N, Zhao J. Speciation of arsenic and chromium in coal and combustion ash by XAFS spectroscopy. Fuel Processing Technology. 1994;39:47-62.

[89] Lowers HA, Breit GN, Foster AL, Whitney J, Yount J, Uddin MN, et al. Arsenic incorporation into authigenic pyrite, Bengal Basin sediment, Bangladesh. Geochimica Et Cosmochimica Acta. 2007;71:2699-717.

[90] Apps JA, Zheng L, Zhang Y, Xu T, Birkholzer JT. Evaluation of potential changes in groundwater quality in response to CO2 leakage from deep geologic storage. Transport in Porous Media. 2010;82:215-46.

[91] Zhou J, Zhuang X, Alastuey A, Querol X, Li J. Geochemistry and mineralogy of coal in the recently explored Zhundong large coal field in the Junggar basin, Xinjiang province, China. International Journal of Coal Geology. 2010;82:51-67.

[92] Xu J, Yu D, Fan B, Zeng X, Lv W, Chen J. Characterization of ash particles from co-combustion with a zhundong coal for understanding ash deposition behavior. Energy & Fuels. 2013;28:678-84.

[93] Ge H, Shen L, Gu H, Song T, Jiang S. Combustion performance and sodium transformation of high-sodium ZhunDong coal during chemical looping combustion with hematite as oxygen carrier. Fuel. 2015;159:107-17.

[94] Jiang S, Shen L, Xin N, Ge H, Gu H. Chemical looping co-combustion of sewage sludge and zhundong coal with natural hematite as oxygen carrier. Energy & Fuels. 2016.

[95] Liu HP, Chen TP, Li Y, Song ZY, Wang SW, Wu SH. Temperature rise characteristics of ZhunDong coal during microwave pyrolysis. Fuel Processing Technology. 2016;148:317-23.

[96] Song G, Qi X, Song W, Lu Q. Slagging characteristics of zhundong coal during circulating fluidized bed gasification. Energy & Fuels. 2016.

[97] Song W, Song G, Qi X, Lu Q. Transformation characteristics of sodium in Zhundong coal under circulating fluidized bed gasification. Fuel. 2016;182:660–7.

[98] Buhre BJP, Elliott LK, Sheng CD, Gupta RP, Wall TF. Oxy-fuel combustion technology for coal-fired power generation. Progress in Energy and Combustion Science. 2005;31:283-307.

[99] Toftegaard MB, Brix J, Jensen PA, Glarborg P, Jensen AD. Oxy-fuel combustion of solid fuels. Progress in Energy and Combustion Science. 2010;36:581-625.

[100] Glarborg P, Bentzen LLB. Chemical effects of a high CO_2 concentration in oxy-fuel combustion of methane. Energy & Fuels. 2007;22:291-6.

[101] Andersson K, Normann F, Filip Johnsson A, Bo L. NO emission during oxy-fuel combustion of lignite. Industrial & Engineering Chemistry Research. 2008;47:1835-45.

[102] Normann F, Andersson K, Bo L, Johnsson F. High-temperature reduction of nitrogen oxides in oxy-fuel combustion. Fuel. 2008;87:3579-85.

[103] Fleig D, Normann F, Andersson K, Johnsson F, Bo L. The fate of sulphur during oxy-fuel combustion of lignite. Energy Procedia. 2009;1:383-90.

[104] Pak PS, Lee YD, Ahn KY, Pak PS, Lee YD, Ahn KY. Characteristics and economic evaluation of a power plant applying oxy-fuel combustion to increase power output and decrease CO_2 emission. Energy. 2010;35:3230-8.

[105] Park SK, Tong SK, Sohn JL, Lee YD. An integrated power generation system combining solid oxide fuel cell and oxy-fuel combustion for high performance and CO_2 capture. Applied Energy. 2011;88:1187-96.

[106] Al-Abbas AH, Naser J, Dodds D. CFD modelling of air-fired and oxy-fuel combustion in a large-scale furnace at Loy Yang A brown coal power station. Fuel. 2012;102:646–65.

[107] Tan Y, Croiset E, Douglas MA, Thambimuthu KV. Combustion characteristics of coal in a mixture of oxygen and recycled flue gas. Fuel. 2006;85:507-12.

[108] Hjärtstam S, Andersson K, Johnsson F, Leckner B. Combustion characteristics of lignite-fired oxy-fuel flames. Fuel. 2009;88:2216-24.

[109] Wang C, Jia L, Tan Y, Anthony EJ. Carbonation of fly ash in oxy-fuel CFB combustion. Fuel. 2008;87:1108-14.

[110] Wu Y, Wang C, Tan Y, Jia L, Anthony EJ. Characterization of ashes from a 100 kW pilot-scale circulating fluidized bed with oxy-fuel combustion. Applied Energy. 2011;88:2940-8.

[111] Wang C, Liu X, Li D, Wu W, Xu Y, Si J. Effect of H_2O and SO_2 on the distribution characteristics of trace

elements in particulate matter at high temperature under oxy-fuel combustion. International Journal of Greenhouse Gas Control. 2014;23:51-60.

[112] Low F, Zhang L. Arsenic emissions and speciation in the oxy-fuel fly ash collected from lab-scale drop-tube furnace. Proceedings of the Combustion Institute. 2013;34:2877-84.

[113] Liu H, Wang C, Sun X, Zhang Y, Zou C. Volatilization of arsenic in coal during isothermal oxy-fuel combustion. Energy & Fuels. 2016;30:3479-87.

[114] Chatain V, Sanchez F, Bayard R, Moszkowicz P, Gourdon R. Effect of experimentally induced reducing conditions on the mobility of arsenic from a mining soil. Journal of Hazardous Materials. 2005;122:119-28.

[115] Yan R, Gauthier D, Flamant G. Possible interactions between As, Se, and Hg during coal combustion. Combustion and Flame. 2000;120:49-60.

[116] Roy B, Choo WL, Bhattacharya S. Prediction of distribution of trace elements under Oxy-fuel combustion condition using Victorian brown coals. Fuel. 2013;114:135-42.

[117] Contreras ML, García-Frutos FJ, Bahillo A. Oxy-fuel combustion effects on trace metals behaviour by equilibrium calculations. Fuel. 2013;108:474-83.

[118] http://www.hsc-chemistry.net/.

[119] Zhuang Y, Pavlish JH. Fate of hazardous air pollutants in oxygen-fired coal combustion with different flue gas recycling. Environmental science & technology. 2012;46:4657-65.

[120] Meij R. Trace element behavior in coal-fired power plants. Fuel Processing Technology. 1994;39:199-217.

[121] Pires M, Querol X. Characterization of Candiota (South Brazil) coal and combustion by-product. International Journal of Coal Geology. 2004;60:57-72.

[122] Song DY, Yin-Juan MA, Qin Y, Wang WF, Zheng CG. Volatility and mobility of some trace elements in coal from Shizuishan Power Plant. Journal of Fuel Chemistry & Technology. 2011;39:328-32.

[123] Aunela-Tapola L, Hatanpää E, Hoffren H, Laitinen T, Larjava K, Rasila P, et al. A study of trace element behaviour in two modern coal-fired power plants : II. Trace element balances in two plants equipped with semi-dry flue gas desulphurisation facilities. Fuel Processing Technology. 1998;55:13-34.

[124] Wang C, Liu X, Li D, Si J, Zhao B, Xu M. Measurement of particulate matter and trace elements from a coal-fired power plant with electrostatic precipitators equipped the low temperature economizer. Proceedings of the Combustion Institute. 2015;35:2793-800.

[125] Li Z, Clemens AH, Moore TA, Gong D, Weaver SD, Eby N. Partitioning behaviour of trace elements in a stoker-fired combustion unit: An example using bituminous coals from the Greymouth coalfield (Cretaceous), New Zealand. International Journal of Coal Geology. 2005;63:98-116.

[126] Clemens AH, Damiano LF, Gong D, Matheson TW. Partitioning behaviour of some toxic volatile elements during stoker and fluidised bed combustion of alkaline sub-bituminous coal. Fuel. 1999;78:1379-85.

[127] Otero-Rey JR, López-Vilariño JM, Moreda-Piñeiro J, Alonso-Rodríguez E, Muniategui-Lorenzo S, López-Mahía P, et al. As, Hg, and Se flue gas sampling in a coal-fired power plant and their fate during coal combustion. Environmental Science & Technology. 2003;37:5262-7.

[128] Reddy MS, Basha S, Joshi HV, Jha B. Evaluation of the emission characteristics of trace metals from coal and fuel oil fired power plants and their fate during combustion. Journal of Hazardous Materials. 2005;123:242–9.

[129] Duan L, Cui J, Jiang Y, Zhao C, Anthony EJ. Partitioning behavior of Arsenic in circulating fluidized bed boilers co-firing petroleum coke and coal. Fuel Processing Technology. 2017;166:107-14.

[130] Ratafia-Brown JA. Major environmental aspects of gasification-based power generation technologies. 2002.

[131] Keefer RF, Sajwan KS. Trace elements in coal and coal combustion residues. CRC Press. 1993.

[132] Foley SF, Barth MG, Jenner GA. Rutile/melt partition coefficients for trace elements and an assessment of the influence of rutile on the trace element characteristics of subduction zone magmas. Geochimica et Cosmochimica Acta. 2000;64:933-8.

[133] Seames WS. The partitioning of trace elements during pulverized coal combustion. Tucson: The University of Arizona; 2000.

[134] Spears DA, Martinez-Tarrazona MR. Trace elements in combustion residues from a UK power station. Fuel. 2004;83:2265-70.

[135] Cotton A, Patchigolla K, Oakey JE. Minor and trace element emissions from post-combustion CO_2 capture from coal: Experimental and equilibrium calculations. Fuel. 2013;117:391-407.

[136] Saqib N, Bäckström M. Trace element partitioning in ashes from boilers firing pure wood or mixtures of solid waste with respect to fuel composition, chlorine content and temperature. Waste Management. 2014;34:2505-19.

[137] Zhou C, Liu G, Fang T, Lam PKS. Investigation on thermal and trace element characteristics during co-combustion biomass with coal gangue. Bioresource Technology. 2014;175:454-62.

[138] Sakulpitakphon T, Hower JC, Trimble AS, Schram WH, Thomas GA. Arsenic and mercury partitioning in fly ash at a Kentucky power plant. Energy & Fuels. 2003;17:1028-33.

[139] Zielinski RA, Foster AL, Meeker GP, Brownfield IK. Mode of occurrence of arsenic in feed coal and its derivative fly ash, Black Warrior Basin, Alabama. Fuel. 2007;86:560-72.

[140] Wang LA, Song ZX, Ding SM, Huang C, University C, Chongqing, et al. Research on the distribution of the particle sizes and leaching characteristics of arsenic and mercury in MSWI fly ash. Journal of Safety & Environment. 2009.

[141] Luo Y, Giammar DE, Huhmann BL, Catalano JG. Speciation of selenium, arsenic, and zinc in class C fly ash. Energy & Fuels. 2011;25:2980-7.

[142] Jin Y, Yuan C, Jiang W, Qi L. Evaluation of bioaccessible arsenic in fly ash by an in vitro method and influence of particle-size fraction on arsenic distribution. Journal of Material Cycles & Waste Management. 2013;15:516-21.

[143] Yuan CG, Jin Y, Wang S. Fractionation and distribution of arsenic in desulfurization Gypsum, Slag and fly ash from a Coal-fired power plant. Fresenius Environmental Bulletin. 2013;22:884-9.

[144] Song C, Xu D, Jiang C, Teng Y, Sun Z, Xu H, et al. The effect of particle size and metal contents on arsenic distribution in coal-fired fly ash. Journal of Thermal Analysis & Calorimetry. 2014;116:1279-84.

[145] Querol X, Alastuey A, Fernández-Turiel J, López-Soler A. Synthesis of zeolites by alkaline activation of ferro-aluminous fly ash. Fuel. 1995;74:1226-31.

[146] Liu G, Zhang H, Gao L, Zheng L, Peng Z. Petrological and mineralogical characterizations and chemical composition of coal ashes from power plants in Yanzhou mining district, China. Fuel Processing Technology. 2004;85:1635-46.

[147] Ratafia-Brown JA. Overview of trace element partitioning in flames and furnaces of utility coal-fired boilers. Fuel Processing Technology. 1994;39:139-57.

[148] Tang Q, Liu G, Zhou C, Sun R. Distribution of trace elements in feed coal and combustion residues from two coal-fired power plants at Huainan, Anhui, China. Fuel. 2013;107:315-22.

[149] Klein DH, Andren AW, Carter JA, Emery JF, Feldman C, Fulkerson W, et al. Pathways of thirty-seven

trace elements through coal-fired power plant. Environmental Science & Technology. 1975;9.

[150] Gladney ES, Small JA, Gordon GE, Zoller WH. Composition and size distribution of in-stack particulate material at a coal-fired power plant. Atmospheric Environment. 1976;10:1071-7.

[151] Kauppinen EI, Pakkanen TA. Coal combustion aerosols: a field study. Environmental Science & Technology. 1990;24:1811-8.

[152] Martinez MR. The fate of trace elements and bulk minerals in pulverized coal combustion in a power station. Fuel Processing Technology. 1996;47:79-92.

[153] Demir I, Hughes RE, Lytle JM, Ho KK. Atmospheric emissions of trace elements at three types of coal-fired power plants. ACS Division of Fuel Chemistry Preprints. 1997.

[154] Sandelin K, Backman R. Trace elements in two pulverized coal-fired power stations. Environmental Science & Technology. 2001:826-34.

[155] Guo X, Zheng CG, Cheng D. Characterization of arsenic emissions from a coal-fired power plant. Energy & fuels. 2006;27:631-4.

[156] Cheng C, Hack P, Chu P, Chang Y, Lin T, Ko C-S, et al. Partitioning of mercury, arsenic, selenium, boron, and chloride in a full-scale coal combustion process equipped with selective catalytic reduction, electrostatic precipitation, and flue gas desulfurization systems. Energy & Fuels. 2009;23:4805-16.

[157] Pandey VC, Singh JS, Singh RP, Singh N, Yunus M. Arsenic hazards in coal fly ash and its fate in Indian scenario. Resources, Conservation and Recycling. 2011;55:819-35.

[158] Córdoba P, Ochoa-Gonzalez R, Font O, Izquierdo M, Querol X, Leiva C, et al. Partitioning of trace inorganic elements in a coal-fired power plant equipped with a wet Flue Gas Desulphurisation system. Fuel. 2012;92:145-57.

[159] Quispe D, Pérez-López R, Silva LFO, Nieto JM. Changes in mobility of hazardous elements during coal combustion in Santa Catarina power plant (Brazil). Fuel. 2012;94:495-503.

[160] Sia S-G, Abdullah WH. Enrichment of arsenic, lead, and antimony in Balingian coal from Sarawak, Malaysia: Modes of occurrence, origin, and partitioning behaviour during coal combustion. International Journal of Coal Geology. 2012;101:1-15.

[161] Hu H, Liu H, Chen J, Li A, Yao H. Speciation transformation of arsenic during municipal solid waste incineration. Proceedings of the Combustion Institute. 2015;35:2883-90.

[162] Linak WP, Peterson TW. Mechanisms governing the composition and size distribution of ash aerosol in a laboratory pulverized coal combustor. Symposium on Combustion. 1988;21:399-410.

[163] Font O, Córdoba P, Leiva C, Romeo LM, Bolea I, Guedea I, et al. Fate and abatement of mercury and other trace elements in a coal fluidised bed oxy combustion pilot plant. Fuel. 2012;95:272-81.

[164] Duan L, Sun H, Jiang Y, Anthony EJ, Zhao C. Partitioning of trace elements, As, Ba, Cd, Cr, Cu, Mn and Pb, in a 2.5MW th pilot-scale circulating fluidised bed combustor burning an anthracite and a bituminous coal. Fuel Processing Technology. 2016;146:1-8.

[165] Neville M. A laboratory study of the effect of coal selection on the amount and composition of combustion generated submicron particles. Combustion Science & Technology. 1990;74:245-65.

[166] Helble JJ. Trace element behavior during coal combustion: results of a laboratory study. Fuel Processing Technology. 1994;39:159-72.

[167] Neville M, Sarofim AF. The stratified composition of inorganic submicron particles produced during coal combustion. Symposium on Combustion. 1982;19:1441-9.

[168] Jiao F, Ninomiya Y, Zhang L, Yamada N, Sato A, Dong Z. Effect of coal blending on the leaching characteristics of arsenic in fly ash from fluidized bed coal combustion. Fuel Processing Technology. 2013;106:769-75.

[169] Helble JJ. A model for the air emissions of trace metallic elements from coal combustors equipped with electrostatic precipitators. Fuel Processing Technology. 2000;63:125-47.

[170] Quann RJ, Neville M, Janghorbani M, Mims CA, Sarofim AF. Mineral matter and trace-element vaporization in a laboratory-pulverized coal combustion system. Environmental Science & Technology. 1982;16(11): 776-781.

[171] Senior CL, Bool III LE, Srinivasachar S, Pease BR, Porle K. Pilot scale study of trace element vaporization and condensation during combustion of a pulverized sub-bituminous coal. Fuel Processing Technology. 2000;63:149-65.

[172] Senior CL, Zeng T, Che J, Ames MR, Sarofim AF, Olmez I, et al. Distribution of trace elements in selected pulverized coals as a function of particle size and density. Fuel Processing Technology. 2000;63:215-41.

[173] Yi H, Hao J, Duan L, Tang X, Ning P, Li X. Fine particle and trace element emissions from an anthracite coal-fired power plant equipped with a bag-house in China. Fuel. 2008;87:2050-7.

[174] Clarke LB, Sloss LL. Trace elements-emissions from coal combustion and gasification: IEA Coal Research; 1992.

[175] Huggins FE. Overview of analytical methods for inorganic constituents in coal. International Journal of Coal Geology. 2002;50:169-214.

[176] Huggins FE, Najih M, Huffman GP. Direct speciation of chromium in coal combustion by-products by X-ray absorption fine-structure spectroscopy. Fuel. 1999;78:233-42.

[177] Tan Y, Mortazavi R, Dureau B, Douglas MA. An investigation of mercury distribution and speciation during coal combustion. Fuel. 2004;83:2229-36.

[178] Chen L, Duan Y, Zhuo Y, Yang L, Zhang L, Yang X, et al. Mercury transformation across particulate control devices in six power plants of China: The co-effect of chlorine and ash composition. Fuel. 2007;86:603-10.

[179] Goodarzi F. Speciation and mass-balance of mercury from pulverized coal fired power plants burning western Canadian subbituminous coals. Journal of Environmental Monitoring. 2004;6:792-8.

[180] Huggins FE, Huffman GP. Modes of occurrence of trace elements in coal from XAFS spectroscopy. International Journal of Coal Geology. 1996;32:31-53.

[181] Goodarzi F, Huggins FE. Speciation of chromium in feed coals and ash byproducts from Canadian power plants burning subbituminous and bituminous coals. Energy & Fuels. 2005;19:2500-8.

[182] Huggins FE, Huffman GP, Kolker A, Mroczkowski SJ, Palmer CA, Finkelman RB. Combined application of XAFS spectroscopy and sequential leaching for determination of arsenic speciation in coal. Energy & Fuels. 2002;16:1167-72.

[183] Huggins FE, Shah N, Huffman GP, Robertson JD. XAFS spectroscopic characterization of elements in combustion ash and fine particulate matter. Fuel Processing Technology. 2000;66:203-18.

[184] Shah P, Strezov V, Stevanov C, Nelson PF. Speciation of arsenic and selenium in coal combustion products. Energy & Fuels. 2007;21:506-12.

[185] Goodarzi F. Mineralogy, elemental composition and modes of occurrence of elements in Canadian feed-coals. Fuel. 2002;81:1199-213.

[186] Goodarzi F, Huggins FE. Monitoring the species of arsenic, chromium and nickel in milled coal, bottom ash and fly ash from a pulverized coal-fired power plant in western Canada. Journal of Environmental

Monitoring. 2001;3:1-6.

[187] López-Antón MA, Díaz-Somoano M, Spears DA, Martínez-Tarazona MR. Arsenic and selenium capture by fly ashes at low temperature. Environmental Science & Technology. 2006;40:3947-51.

[188] Yu-Hu LI, Liu ZH, Zhao ZW, Qi-Hou LI, Liu ZY, Li Z. Determination of arsenic speciation in secondary zinc oxide and arsenic leachability. Transactions of Nonferrous Metals Society of China. 2012;22:1209-16.

[189] Bartoňová L. Effect of CaO, Al_2O_3 and Fe_2O_3 in coal ash on the retention of acid-forming elements during coal combustion. Wseas Transactions on Power Systems. 2014;9:486-94.

[190] Harrison WTA. Synthetic mansfieldite, $AlAsO_4 \cdot 2H_2O$. Acta Cryst. 2000;56:421.

[191] Gopal R, Calvo C. Crystal Structure of $Ca_3(AsO_4)_2$. Canadian Journal of Chemistry. 2011;49:1036-46.

[192] Pertlik F. Die Kristallstruktur von $Ca_2As_2O_7$. Monatshefte Fuer Chemie/chemical Monthly. 1980;111:399-405.

[193] Raeva AA, Dongari N, Artemyeva AA, Kozliak EI, Pierce DT, Seames WS. Experimental simulation of trace element evolution from the excluded mineral fraction during coal combustion using GFAAS and TGA–DSC. Fuel. 2014;124:28-40.

[194] Germani MS, Zoller WH. Vapor-phase concentrations of arsenic, selenium, bromine, iodine, and mercury in the stack of a coal-fired power plant. Environmental Science & Technology. 1988;22:1079-85.

[195] Attalla M, Morgan S, Riley K. Trace element deportment in combustion processes. 2004.

[196] Vejahati F, Xu Z, Gupta R. Trace elements in coal: Associations with coal and minerals and their behavior during coal utilization – A review. Fuel. 2010;89:904-11.

[197] Tang L, Gupta R, Sheng C, Wall T. The char structure characterization from the coal reflectogram. Fuel. 2005;84:1268-76.

[198] Buhre BJP, Hinkley JT, Gupta RP, Nelson PF, Wall TF. Fine ash formation during combustion of pulverised coal–coal property impacts. Fuel. 2006;85:185-93.

[199] Takuwa T, Mkilaha ISN, Naruse I. Mechanisms of fine particulates formation with alkali metal compounds during coal combustion. Fuel. 2006;85:671-8.

[200] Li G, Li S, Huang Q, Yao Q. Fine particulate formation and ash deposition during pulverized coal combustion of high-sodium lignite in a down-fired furnace. Fuel. 2015;143:430-7.

[201] Xiao Z, Shang T, Zhuo J, Yao Q. Study on the mechanisms of ultrafine particle formation during

high-sodium coal combustion in a flat-flame burner. Fuel. 2016;181:1257-64.

[202] Buhre BJP, Hinkley JT, Gupta RP, Wall TF, Nelson PF. Submicron ash formation from coal combustion. Fuel. 2005;84:1206-14.

[203] Zhang L, Ninomiya Y, Yamashita T. Formation of submicron particulate matter (PM1) during coal combustion and influence of reaction temperature. Fuel. 2006;85:1446-57.

[204] Quann RJ, Sarofim AF. A scanning electron microscopy study of the transformations of organically bound metals during lignite combustion. Fuel. 1986;65:40-6.

[205] Gupta RP, Yan LY, Gupta SK, Wall TF, Kiga T, Watanabe S. CCSEM analysis of minerals in coal and thermal performance of PC-fired boilers. Clean Air. 2005;6:157-70.

[206] Senior CL, Helble JJ, Sarofim AF. Emissions of mercury, trace elements, and fine particles from stationary combustion sources. Fuel Processing Technology. 2000;65:263-88.

[207] Chakraborti N, Lynch DC. Thermodynamic Analysis of the As–S–O Vapor System. Canadian Metallurgical Quarterly. 1985;24:39-45(7).

[208] Díaz-Somoano M, Martínez-Tarazona MR. Trace element evaporation during coal gasification based on a thermodynamic equilibrium calculation approach. Fuel. 2003;82:137-45.

[209] Konttinen J, Backman R, Hupa M, Moilanen A, Kurkela E. Trace element behavior in the fluidized bed gasification of solid recovered fuels–A thermodynamic study. Fuel. 2013;106:621-31.

[210] Singh TS, Pant KK. Equilibrium, kinetics and thermodynamic studies for adsorption of As(III) on activated alumina. Separation and Purification Technology. 2004;36:139-47.

[211] Linak WP, Wendt JOL. Toxic metal emissions from incineration: mechanisms and control. Progress in Energy and Combustion Science. 1993;19:145-85.

[212] Linak WP, Wendt JOL. Trace metal transformation mechanisms during coal combustion. Fuel Processing Technology. 1994;39:173-98.

[213] Davis SB, Gale TK, Wendt JOL, Linak WP. Multicomponent coagulation and condensation of toxic metals in combustors. Symposium on Combustion. 1998;27:1785-91.

[214] James DW, Krishnamoorthy G, Benson SA, Seames WS. Modeling trace element partitioning during coal combustion. Fuel Processing Technology. 2014;126:284-97.

[215] Zeng T, Sarofim AF, Senior CL. Vaporization of arsenic, selenium and antimony during coal combustion.

Combustion and Flame. 2001;126:1714–24.

[216] Raeva AA, Pierce DT, Seames WS, Kozliak EI. A method for measuring the kinetics of organically associated inorganic contaminant vaporization during coal combustion. Fuel Processing Technology. 2011;92:1333-9.

[217] Raask E. The mode of occurrence and concentration of trace elements in coal. Progress in Energy & Combustion Science. 1985;11:97-118.

[218] Tomeczek J, Palugniok H. Kinetics of mineral matter transformation during coal combustion. Fuel. 2002;81:1251-8.

[219] Baxter LL. Char fragmentation and fly ash formation during pulverized-coal combustion. Combustion & Flame. 1992;90:174-84.

[220] Wang S, Zhang L, Li G, Wu Y, Hao J, Pirrone N, et al. Mercury emission and speciation of coal-fired power plants in China. Atmospheric Chemistry and Physics. 2010;10:1183-92.

[221] Deng S, Shi Y, Liu Y, Zhang C, Wang X, Cao Q, et al. Emission characteristics of Cd, Pb and Mn from coal combustion: Field study at coal-fired power plants in China. Fuel Processing Technology. 2014;126:469-75.

[222] Itskos G, Itskos S, Koukouzas N. Size fraction characterization of highly-calcareous fly ash. Fuel Processing Technology. 2010;91:1558-63.

[223] Chen L, Dick WA, Nelson S. Flue gas desulfurization products as sulfur sources for alfalfa and soybean. Agronomy Journal. 2005;97:265-71.

[224] Álvarez-Ayuso E, Querol X, Tomás A. Environmental impact of a coal combustion-desulphurisation plant: Abatement capacity of desulphurisation process and environmental characterisation of combustion by-products. Chemosphere. 2006;65:2009-17.

[225] Wang C, Zhang Y, Shi Y, Liu H, Zou C, Wu H, et al. Research on collaborative control of Hg, As, Pb and Cr by electrostatic-fabric-integrated precipitator and wet flue gas desulphurization in coal-fired power plants. Fuel. 2017;210:527-34.

[226] Álvarez-Ayuso E, Querol X, Ballesteros JC, Giménez A. Risk minimisation of FGD gypsum leachates by incorporation of aluminium sulphate. Science of the Total Environment. 2008;406:69-75.

[227] Vassilev SV, Vassileva CG. Geochemistry of coals, coal ashes and combustion wastes from coal-fired power stations. Fuel Processing Technology. 1997;51:19-45.

[228] Ito S, Yokoyama T, Asakura K. Emissions of mercury and other trace elements from coal-fired power plants in Japan. Science of the Total Environment. 2006;368:397-402.

[229] Kuprianov VI, Tanetsakunvatana V. Assessment of gaseous, PM and trace element emissions from a 300-MW lignite-fired boiler unit for various fuel qualities. Fuel. 2006;85:2171-9.

[230] Häsänen E, Aunela-Tapola L, Kinnunen V, Larjava K, Mehtonen A, Salmikangas T, et al. Emission factors and annual emissions of bulk and trace elements from oil shale fueled power plants. Science of the Total Environment. 1997;198:1-12.

[231] Nriagu JO, Pacyna JM. Quantitative assessment of worldwide contamination of air, water and soils by trace metals. Nature. 1988;333:134-9.

[232] Izquierdo M, Querol X. Leaching behaviour of elements from coal combustion fly ash: An overview. International Journal of Coal Geology. 2012;94:54-66.

[233] Wang W, Yong Q, Song D, Wang K. Column leaching of coal and its combustion residues, Shizuishan, China. International Journal of Coal Geology. 2008;75:81-7.

[234] Baba A, Gurdal G, Sengunalp F. Leaching characteristics of fly ash from fluidized bed combustion thermal power plant: Case study: Çan (Çanakkale-Turkey). Fuel Processing Technology. 2010;91:1073-80.

[235] Otero-Rey JR, Mato-Fernández MJ, Moreda-Piñeiro J, Alonso-Rodríguez E, Muniategui-Lorenzo S, López-Mahía P, et al. Influence of several experimental parameters on As and Se leaching from coal fly ash samples. Analytica Chimica Acta. 2005;531:299-305.

[236] Tian H, Liu K, Zhou J, Lu L, Hao J, Qiu P, et al. Atmospheric emission inventory of hazardous trace elements from China's coal-fired power plants: temporal trends and spatial variation characteristics. Environmental Science & Technology. 2014;48:3575-82.

[237] Mahuli S, Agnihotri R, Chauk S, Ghosh-Dastidar A, Fan LS. Mechanism of arsenic sorption by hydrated lime. Environmental Science & Technology. 1997;31:3226-31.

[238] López-Antón MA, Díaz-Somoano M, Fierro JLG, Martínez-Tarazona MR. Retention of arsenic and selenium compounds present in coal combustion and gasification flue gases using activated carbons. Fuel Processing Technology. 2007;88:799-805.

[239] Zhang Y, Wang C, Liu H. Experiment and mechanism research on gas-phase As_2O_3 adsorption of Fe_2O_3/γ-Al_2O_3. Fuel. 2016;181:1034-40.

[240] Rupp EC, Granite EJ, Stanko DC. Laboratory scale studies of Pd/γ-Al_2O_3 sorbents for the removal of trace contaminants from coal-derived fuel gas at elevated temperatures. Fuel. 2013;108:131-6.

[241] Davidson R, Clarke L. Trace elements in coal. Fuel & Energy Abstracts. 1996;37:230-.

[242] Wouterlood H, Bowling K. Removal and recovery of arsenious oxide from flue gases. Environmental Science & Technology. 1979;13:93-7.

[243] Mitsui Y, Imada N, Kikkawa H, Katagawa A. Study of Hg and SO_3 behavior in flue gas of oxy-fuel combustion system. International Journal of Greenhouse Gas Control. 2011;5:S143-S50.

[244] Wang C, Zhang Y, Liu H. Experimental and mechanism study of gas-phase arsenic adsorption over Fe_2O_3/γ-Al_2O_3 sorbent in oxy-Fuel combustion flue gas. Industrial & Engineering Chemistry Research. 2016;55.

[245] Granite EJ, And HWP, Hargis RA. Novel Sorbents for Mercury Removal from Flue Gas. Industrial & Engineering Chemistry Research. 2011;39:1020-9.

Review of arsenic behavior during coal combustion: Volatilization, transformation, emission and removal technologies

Wang, Chunbo

2018-04-17

Chunbo Wang, Huimin Liu, Yue Zhang, Chan Zou, Edward J. Anthony, Review of arsenic behavior during coal combustion: Volatilization, transformation, emission and removal technologies, Progress in Energy and Combustion Science, Volume 68, September 2018, Pages 1-28

https://doi.org/10.1016/j.pecs.2018.04.001